AN INVESTIGATION OF THE INFLUENCE OF CIRCUIT PARAMETERS ON THE OUTPUT WAVESHAPE OF A TUNNEL DIODE OSCILLATOR

A THESIS

Presented to

The Faculty of the Graduate Division

by

Robert David Shults

In Partial Fulfillment

of the Requirements for the Degree

Master of Science in Electrical Engineering

Georgia Institute of Technology

June, 1963

AN INVESTIGATION OF THE INFLUENCE OF CIRCUIT PARAMETERS ON THE OUTPUT WAVESHAPE OF A TUNNEL DIODE OSCILLATOR

Approved:

Dr. W. B. Jones, Jr. (Chairman)

Dr. J. L. Hammond, Jr.

Dr. J. T. Wang

Date Approved by Chairman: May 23, 1963

In presenting the dissertation as a partial fulfillment of the requirements for an advanced degree from the Georgia Institute of Technology, I agree that the Library of the Institution shall make it available for inspection and circulation in accordance with its regulations governing materials of this type. I agree that permission to copy from, or to publish from, this dissertation may be granted by the professor under whose direction it was written, or, in his absence, by the dean of the Graduate Division when such copying or publication is solely for scholarly purposes and does not involve potential financial gain. It is understood that any copying from, or publication of, this dissertation which involves potential financial gain will not be allowed without written permission.

_____

ACKNOWLEDGMENTS

The author wishes to thank his thesis advisor, Dr. W. B. Jones, Jr., for his suggestion of the problem and for his continued guidance and encouragement during the course of the investigation. At the same time, special thanks are due to the other members of the reading committee, Dr. J. L. Hammond and Dr. J. T. Wang, for their constructive criticisms in the preparation of the manuscript. Appreciation is also expressed to Mr. R. S. Johnson for his advice and suggestions in the preparation of the analog computer program.

TABLE OF CONTENTS

TABLE OF CONTENTS (Continued)

LIST OF ILLUSTRATIONS

Figure Page

SUMMARY

A detailed analysis of a tunnel diode oscillator inevitably requires the solution of a nonlinear differential equation describing its operation. In the past, the volt-ampere characteristic of a device which displays negative dynamic resistance in a reasonably symmetrical N-type curve has been described by a simple third order polynomial. For example, the characteristic of the tetrode vacuum tube is usually described by the simple expression $i = - ae + be^3$. Because of the simplicity of the approximating polynomial used to describe the tetrode, van der Pol was able to solve the nonlinear differential equation which describes the tetrode oscillator. The original work published by van der Pol in 1934 has long since become a classic in the field and has been the inspiration for numerous researches on nonlinear oscillations.

The analysis of a tunnel diode oscillator is complicated by the fact that the volt-ampere characteristic of a tunnel diode is grossly asymmetrical about the region of negative dynamic resistance and cannot be approximated by a simple polynomial. It has been the purpose of this investigation to obtain, without the use of an approximating polynomial, the solution to the nonlinear differential equation which describes a tunnel diode oscillator. The characteristic of the solution which has been of primary interest is the waveshape of the steady-state output and how it is influenced by the different circuit parameters.

The nonlinear equation which describes the tunnel diode oscillator used was found to be

$$\frac{d^2e}{dt^2} + \frac{R}{L}\frac{de}{dt} + \frac{1}{LC}e + \frac{1}{C}\frac{d}{dt}\left[f(e)\right] + \frac{R}{LC}\left[f(e)\right] = 0 ,$$

where f(e) is the nonlinear function which represents the tunnel diode volt-ampere characteristic.

The oscillator was simulated on an analog computer, and the computer was programmed in phase-plane variables. The solution to the oscillator equation was then presented by the computer in graphical form as a phase trajectory together with a recording of the instantaneous output waveshape.

The experimental results are reviewed with major emphasis on the near-sinusoidal mode of operation. The necessary conditions for near-sinusoidal operation are derived in terms of the circuit parameters of interest, namely the impedance level, circuit Q, and bias point.

It is shown that, if the circuit Q and bias point are fixed, the waveshape can be made more nearly sinusoidal by lowering the impedance level.

It is likewise shown that, if the impedance level and bias point are fixed, the waveshape is improved by lowering the circuit Q.

The effect of the bias point on the circuit operation is reviewed in terms of the value of the negative incremental conductance presented by the diode as a function of the bias voltage. In addition, the role of the asymmetry of the diode characteristic is considered, and as a result the bias point is shown to be a controlling factor in whether or not sustained oscillations are possible and, if so, how the steady-state amplitude is limited and the waveform distorted.

Finally, the overall effects of the circuit parameters are considered from the system-root point of view, and it is shown that the results previously obtained all lead in the same direction: improvement in the waveshape is made by adjusting the circuit parameters in such a way as to place the system roots closer to the $j\omega$-axis. Examples are given to illustrate the effect of each parameter on the waveshape and a final example is given to show the almost perfect sinusoidal waveform which may be obtained by adjusting all three parameters simultaneously.

CHAPTER I

INTRODUCTION

Since the development of the Esaki or tunnel diode in 1957, there has been a widespread and rapidly growing interest in its application. The tunnel diode, basically a negative resistance device, is ideally suited for use in logic and switching circuits, amplifiers, and two-terminal or negative resistance oscillators.

This investigation is concerned with the specific application of the tunnel diode as a negative resistance oscillator.

There is an abundance of classical literature dealing with the theory of negative resistance oscillators. One of the most famous papers on this subject is that by van der Pol describing the operation of the tetrode oscillator (1). This work, in which van der Pol took into account the nonlinearity of the tube characteristic, resulted in the well known van der Pol nonlinear differential equation. Since van der Pol published his paper, many workers have investigated the properties of the equation, resulting in numerous contributions to the theory of nonlinear oscillations in general.

One of the key points in the development of van der Pol's equation is that the E-I characteristic of the tetrode, shown in Figure 1(a), is reasonably symmetrical about the center of the range over which it exhibits dynamic negative resistance. In this range, the tube characteristic may be closely approximated by a simple third order polynomial. Van der Pol used the approximating polynomial shown in Figure 1(b) to derive an

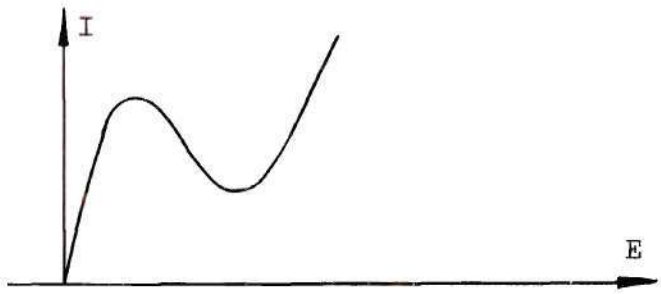

Figure 1(a). General Characteristic of the Tetrode Vacuum Tube.

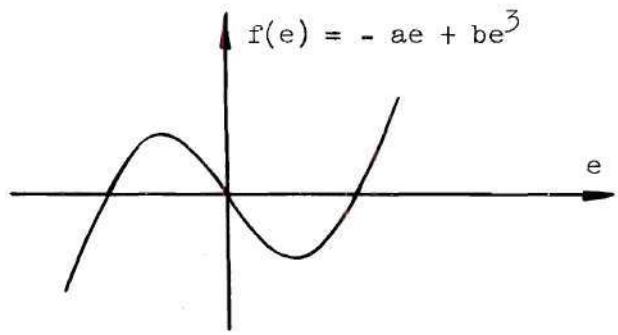

Figure 1(b). Polynomial Representation About the Center of the Negative Resistance Region Used by Van der Pol.

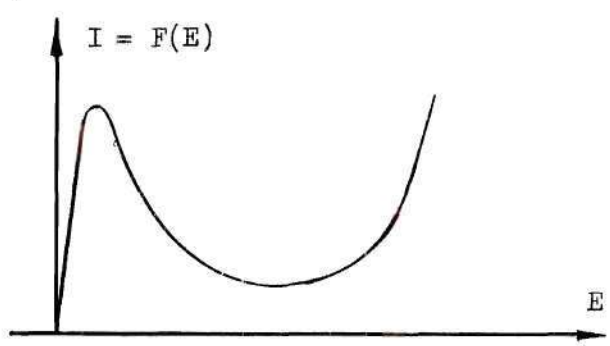

Figure 1(c). Tunnel Diode Static Terminal Volt-Ampere Characteristic.

equation in which the terms describing the nonlinearity are displayed as explicit functions of the dependent variable. For this reason, he was able to solve the equation analytically as well as graphically.

The E-I characteristic of the tunnel diode, shown in Figure 1(c), is markedly nonsymmetrical about any point in its range of dynamic negative resistance. This makes it very difficult to use a polynomial to approximate the diode's characteristic over the range of interest. Even if an approximating polynomial were used, it would be very unwieldy. With this in mind, it appears that any reasonable analysis of a tunnel diode oscillator would have to be one depending on a graphical technique such as phase-plane analysis or some other allied procedure.

It is the purpose of this investigation to obtain a solution to the equation describing a tunnel diode oscillator and to determine the influence of the various oscillator circuit parameters on that solution. The characteristic of the solution on which the greatest attention will be focused is the waveshape of the steady-state output of the tunnel diode oscillator.

A similar problem has been investigated by Docherty and Aitchison (2) using different techniques than those which are employed in this investigation. Though their work was less complete, their conclusions are similar to those reached as a result of this investigation.

CHAPTER II

TUNNEL DIODE OSCILLATOR THEORY

Basic Oscillator Circuits

The tunnel diode, when biased in its region of negative dynamic resistance, may be represented by the equivalent circuit of Figure 2.[1] The series inductance, L_s, arises from the leads of the package and is usually very low. A small series resistance, R_s, is present and represents the bulk resistance of the semiconductor material. The capacitance, C_d, represents the capacity of the p-n junction of the diode. The negative resistance, $\rho(= -R_d)$, represents the negative dynamic resistance of the diode and, for small signals, is given by the reciprocal of the slope of the static E-I characteristic shown in Figure 1(c).

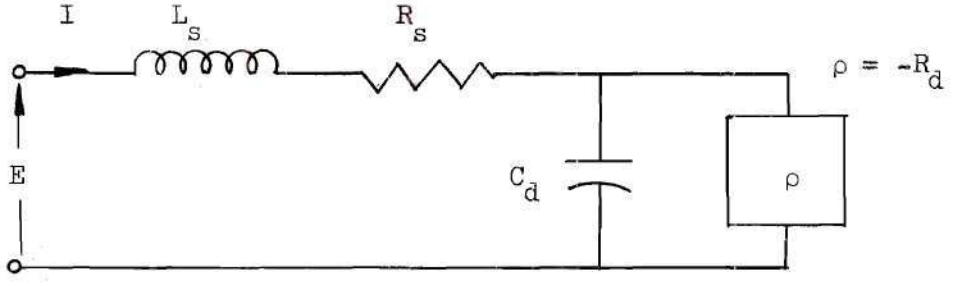

Figure 2. Equivalent Circuit of the Tunnel Diode when Biased in the Region of Negative Resistance.

Considering the equivalent circuit of Figure 2, a negative resistance oscillator is easily constructed as shown in Figure 3(a) (3). Assuming perfect by-passing by C_{bp}, the incremental equivalent circuit

---

[1] See Appendix A for typical values of the diode parameters.

is shown in Figure 3(b).

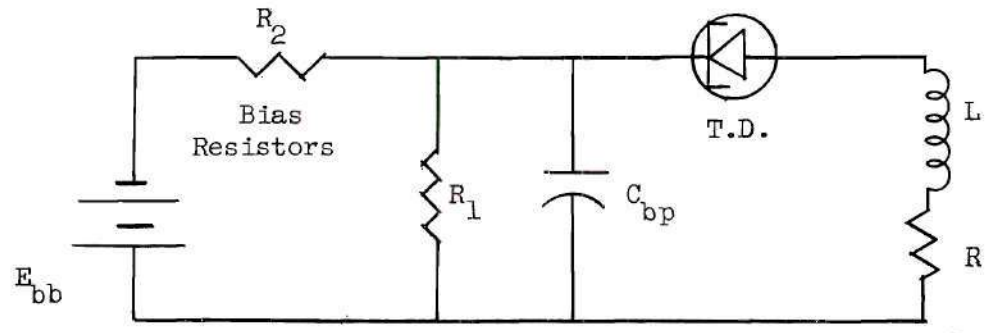

Figure 3(a). Simple Oscillator Circuit.

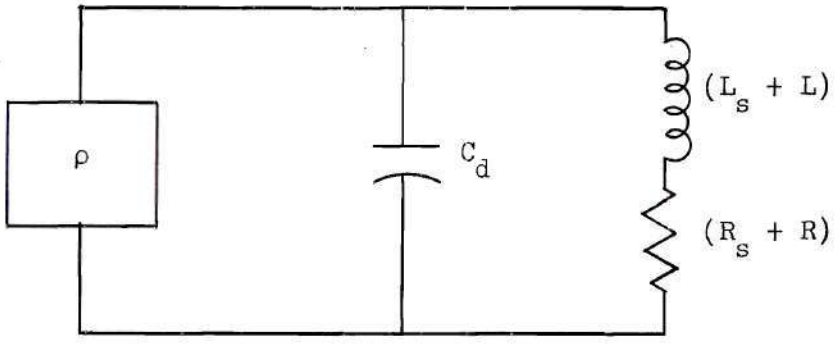

Figure 3(b). Incremental Equivalent Circuit of Figure 3(a).

Another circuit which has better frequency stability and is more easily adjusted in frequency, Q, and impedance level, is shown in Figure 4(a) (4). The incremental equivalent circuit, assuming perfect by-passing by C_{bp}, is shown in Figure 4(b).

During the course of this work, a circuit of the type shown in Figure 4 was used because of its inherent advantages over the simpler type shown in Figure 3. The schematic of the practical oscillator circuit which was used is shown below in Figure 5. The component values shown are chosen so that the oscillator operates near 1 Mcps.

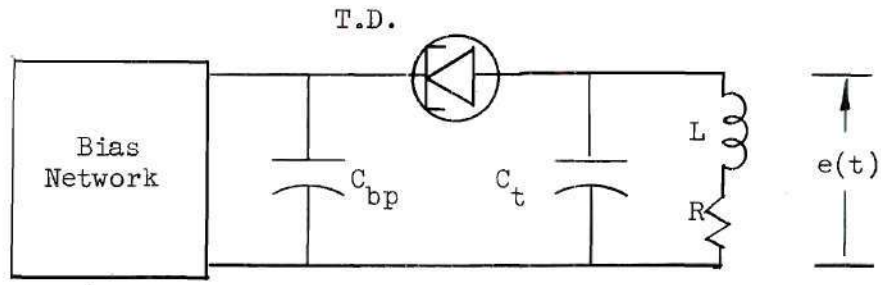

Figure 4(a). Basic Oscillator Circuit.

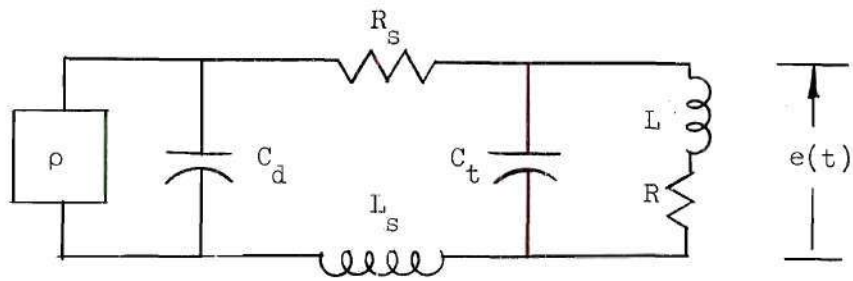

Figure 4(b). Incremental Equivalent Circuit of Figure 4(a).

For application as an oscillator, the diode must be biased in its region of negative resistance. For the operating point to be fixed in this region, it is required that the total series resistance of the DC equivalent circuit (composed of the Thevenin resistance of the bias circuit and the coil resistance) be less than the magnitude of the negative resistance of the diode. If this is the case, the DC load line will then intersect the diode characteristic at only one point, as shown in Figure 6.

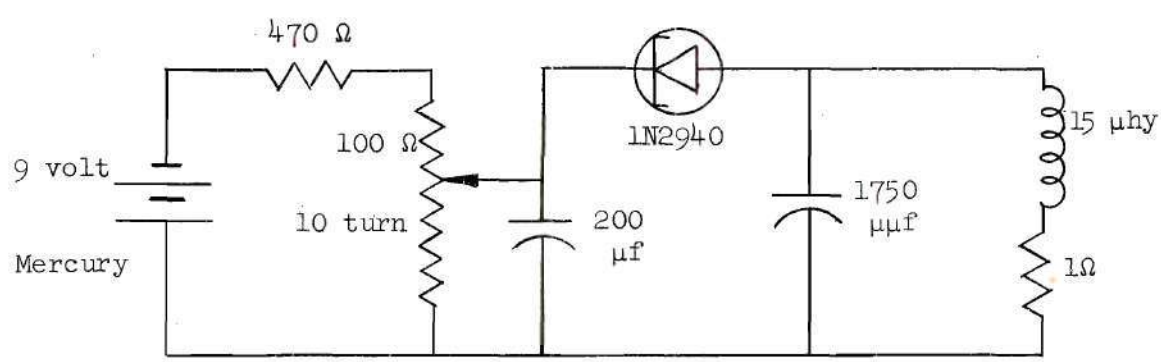

Figure 5. Practical Oscillator Circuit.

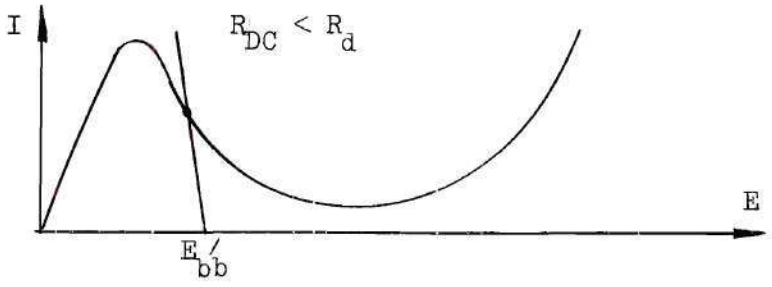

Figure 6. Suitable DC Load Line.

If the total DC resistance of the circuit is increased, the slope of the load line will approach that of the diode characteristic in the negative resistance region. If the DC resistance is greater than the magnitude of the negative resistance of the diode, then the slope of the load line is less than that of the diode characteristic, and intersections can occur at one or three points, depending on E'_{bb} the Thevenin voltage of the bias network, as shown in Figure 7. A load line which intersects the characteristic in the negative resistance region, such as point 3 in Figure 7, will also intersect the characteristic at two other points. It has been shown (5) that the presence of reactive elements in the circuit causes point 3 to be one of unstable equilibrium, and the diode can then only "switch" between the stable points 4 and 5, making it unsuitable

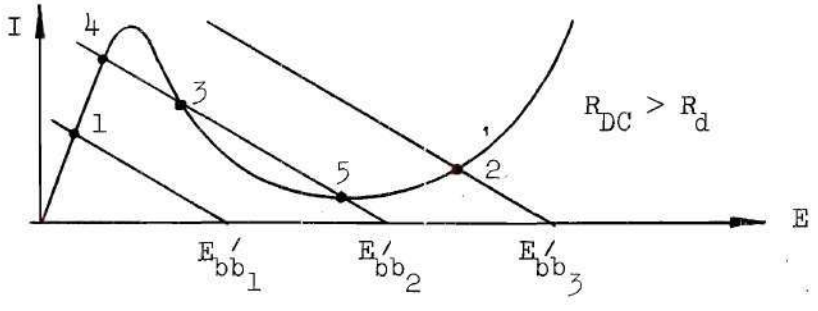

Figure 7. Unsuitable DC Load Lines.

for application as an oscillator if biased in this manner.

Linear Methods of Analysis

Linear Analysis in the Complex Frequency Plane

An analysis of the equivalent circuit of Figure 4(b) is considerably simplified by the assumption that the series inductance and resistance of the diode are negligible. For the diodes used (GE 1N2940) these parameters are small and are considered as negligible in all further analysis.

With the assumption of negligible L_s and R_s, the equivalent circuit of the oscillator reduces to that shown in Figure 8. The equivalent capacitance, C, is now the sum of the tank capacitance, C_t, and the diode junction capacitance C_d.

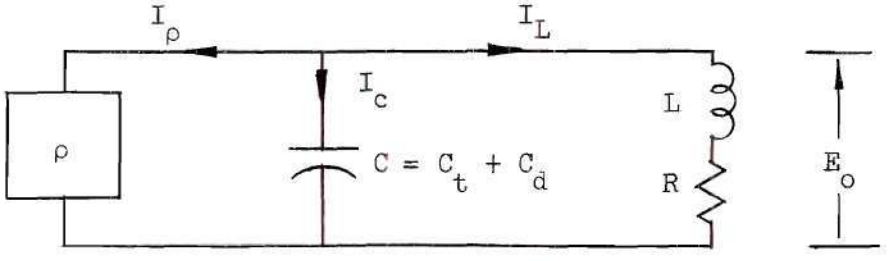

Figure 8. Simplified Equivalent Circuit.

A small signal analysis of the circuit of Figure 8 may be made by investigating the s-plane roots of the equation describing the oscillator. The single node equation which describes the circuit of Figure 8 is

$$I_\rho + I_c + I_L = 0 , \qquad (1)$$

or

$$E_o \left(\frac{1}{\rho} + Cs + \frac{1}{Ls + R}\right) = 0 . \tag{2}$$

The only non-trivial solution is for

$$\left(\frac{1}{\rho} + Cs + \frac{1}{Ls + R}\right) = 0 . \tag{3}$$

Rewriting equation (3) gives

$$\frac{Ls + R + \rho(Ls + R)Cs + \rho}{\rho(Ls + R)} = 0 . \tag{4}$$

The system roots may now be found by equating the numerator of equation (4) to zero. Therefore, the resulting equation to be solved is

$$s^2 + \left(\frac{L + \rho RC}{\rho LC}\right)s + \left(\frac{R + \rho}{\rho LC}\right) = 0 . \tag{5}$$

The roots of the system are then

$$s_1, s_2 = -\frac{1}{2}\left(\frac{L + \rho RC}{\rho LC}\right) \pm \sqrt{\frac{1}{4}\left(\frac{L + \rho RC}{\rho LC}\right)^2 - \left(\frac{R + \rho}{\rho LC}\right)} . \tag{6}$$

For sinusoidal operation at constant amplitude, the s-plane roots must be complex conjugates on the $j\omega$-axis, therefore the real part of the roots must be zero. This condition requires that

$$L + \rho RC = 0 . \tag{7}$$

From the definition of the diode parameters, ρ may alternately be expressed as

$$\rho = -R_d = -\frac{1}{G_d} , \tag{8}$$

where R_d and G_d are positive numbers. Substitution of equation (8) in equation (7) yields the restriction on the circuit parameters for sinusoidal operation

$$R = \frac{L}{C} G_d \quad . \tag{9}$$

With the restriction of equation (9), the roots are of the form

$$s_1, s_2 = \pm j \omega_o \quad , \tag{10}$$

where ω_o is the frequency of oscillation and is given by

$$\omega_o = \left[\frac{R + \rho}{\rho LC}\right]^{1/2} = \frac{1}{\sqrt{LC}} \left[1 - \frac{R^2 C}{L}\right]^{1/2} \quad . \tag{11}$$

The natural frequency of the circuit of Figure 8 in the lossless case ($R = 0$) is $\omega_n = 1/\sqrt{LC}$. For a high-Q circuit the coil resistance, R, would be small, and the frequency of oscillation, ω_o, would be very near ω_n, which is determined primarily by the external resonator parameters C_t and L.

For the oscillator to be self-starting, the system roots must initially be located in the right half of the s-plane. The output waveshape will then depend on the migration of the roots during the build up of oscillations. If the roots move toward the jω-axis, the output approaches a pure sinusoid. If the system roots migrate further into the right-half-plane, the build up soon involves the nonlinearity of the characteristic. At this point, the output is far from sinusoidal and is known as a relaxation oscillation. The transition from nearly sinusoidal

to relaxation oscillations is smooth, and there is no clear cut dividing line to separate the two cases. An extreme case of relaxation oscillations is one in which the system roots have coalesced and fall on the positive real axis in the s-plane. A relaxation oscillator is sometimes defined as a system whose s-plane roots are positive, pure, real, and simple (6).

The position of the s-plane roots can be used to gain insight into the nonlinear behavior of the oscillator as will be shown when the results of the more difficult nonlinear solution are discussed in a later section.

Linear Differential Equation Analysis

One of the most useful methods of gaining an insight into the fundamental mechanism of a negative resistance oscillator is to analyze the basic circuit of Figure 8 in terms of a linear differential equation for the instantaneous output voltage. For convenience, the basic circuit is repeated in Figure 9 with the instantaneous output voltage and branch currents shown.

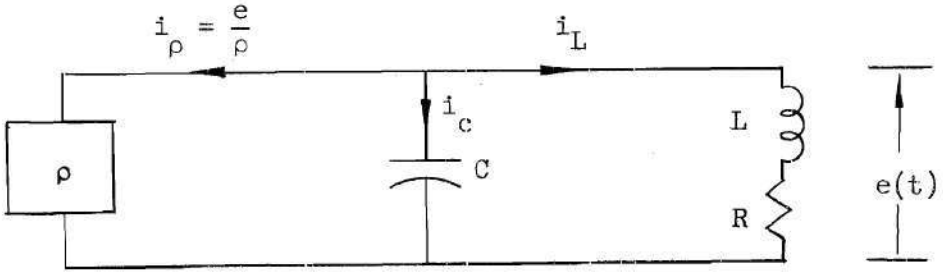

Figure 9. Basic Oscillator Circuit.

The single node equation which describes the circuit is

$$i_L = - i_c - i_\rho$$

$$= - C \frac{de}{dt} - \frac{e}{\rho} . \qquad (12)$$

The instantaneous output voltage is given by

$$e(t) = L \frac{di_L}{dt} + R\, i_L \,. \tag{13}$$

The use of equation (12) and the relation $\rho = -1/G_d$ in equation (13) yields

$$\frac{d^2e}{dt^2} + \frac{1}{LC}\,(RC - L\,G_d)\frac{de}{dt} + \frac{1}{LC}\,(1 - R\,G_d)e = 0 \,. \tag{14}$$

Equation (14) is of the general form

$$\frac{d^2e}{dt^2} + 2\alpha \frac{de}{dt} + \omega_o^2\, e = 0 \,, \tag{15}$$

where

$$\alpha = \frac{1}{2LC}\,(RC - L\,G_d) \,, \tag{16}$$

and

$$\omega_o = \frac{1}{\sqrt{LC}}\left[1 - R\,G_d\right]^{1/2} \,. \tag{17}$$

The oscillatory solution for equation (15) is of the general form

$$e(t) = Ae^{-\alpha t}\cos\,(\beta t + \theta) \,, \tag{18}$$

where

$$\beta = \left[\omega_o^2 - \alpha^2\right]^{1/2} \,. \tag{19}$$

In a passive system, the damping constant, α, is always a positive number which means that the oscillations will decay with time.

The principle behind a negative resistance oscillator is that the damping constant as given by equation (16) can, through the correct choice of circuit parameters, be made to equal zero. If this is the case, then $\beta = \omega_o$, and the circuit equation takes the form

$$\frac{d^2e}{dt^2} + \omega_o^2 e = 0 , \tag{20}$$

and the solution is of the form

$$e(t) = A \cos (\omega_o t + \theta) . \tag{21}$$

This is an oscillation at the angular frequency ω_o with the constant amplitude A.

The restriction on the circuit parameters for $\alpha = 0$ is found from equation (16) to be

$$RC - L G_d = 0 . \tag{22}$$

Therefore,

$$R = \frac{L}{C} G_d . \tag{23}$$

For this case, the frequency of oscillation becomes

$$\omega_o = \frac{1}{\sqrt{LC}} \left[1 - \frac{R^2C}{L} \right]^{1/2} , \tag{24}$$

and the results of equations (23) and (24) are identically those found in equations (9) and (11) of the preceding section.

Alternate Quasi-Linear Analysis

An alternate approximate approach is useful in explaining the behavior of the oscillator in the quasi-linear near-sinusoidal state of operation. For a high-Q circuit, the tank circuit of Figure 9 may be closely approximated by the equivalent form shown below in Figure 10. The equivalent parallel conductance G represents the losses of the system

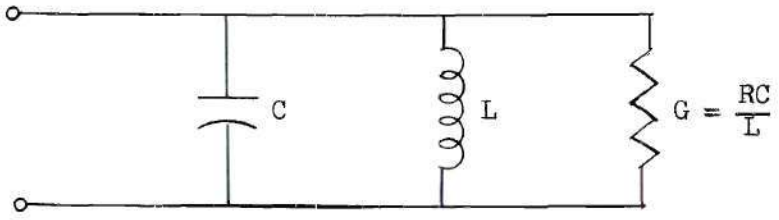

Figure 10. Equivalent Tank Circuit.

and also represents the input admittance of the circuit at the natural frequency $\omega_n = 1/\sqrt{LC}$. The alternate equivalent form of the basic oscillator circuit is shown in Figure 11. Again assuming that ρ is

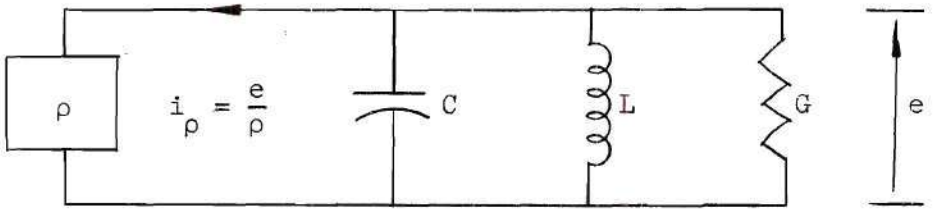

Figure 11. Alternate Equivalent Basic Oscillator Circuit.

essentially constant, the node equation describing the circuit of Figure 11 is

$$C\frac{de}{dt} + \left(G + \frac{1}{\rho}\right)e + \frac{1}{L}\int e\,dt = 0 . \qquad (25)$$

This may be rewritten as

$$\frac{d^2e}{dt^2} + \frac{1}{C}(G - G_d)\frac{de}{dt} + \frac{1}{LC}e = 0 . \tag{26}$$

The quasi-linear equation (26) is essentially the same as equation (14) the only difference being the coefficient of e. In equation (14), the coefficient of e is

$$\omega_o^2 = \frac{1}{LC} - \frac{R}{LC}G_d . \tag{27}$$

In equation (26) the coefficient of e is

$$\omega_n^2 = \frac{1}{LC} . \tag{28}$$

For the high-Q case, $\frac{1}{LC} >> \frac{RG_d}{LC}$, and $\omega_n^2 \cong \omega_o^2$. The quasi-linear equation (26) has two roots which characterize the time response.

$$m_1, m_2 = -\frac{1}{2C}(G - G_d) \pm j\sqrt{\frac{1}{LC} - \frac{1}{4C^2}(G - G_d)^2}$$
$$= \alpha \pm j\beta \tag{29}$$

For a growing oscillation, the following conditions must hold:

$$\alpha > 0 \tag{30}$$

$$\text{with } \beta \text{ real.} \tag{31}$$

For the condition (30) to be satisfied, it must be true that

$$G_d > G . \tag{32}$$

The inequality (32) dictates that the slope of the dynamic load line, - G, must be less than the slope of the diode characteristic, $- G_d$.

This means that the dynamic load line will intersect the diode characteristic at two points other than the bias point, as shown in Figure 12.

For the boundary condition of $G = G_d$, the dynamic load line is exactly tangent to the diode characteristic at the bias point, and ideally this condition corresponds to a perfect sinusoidal waveshape.

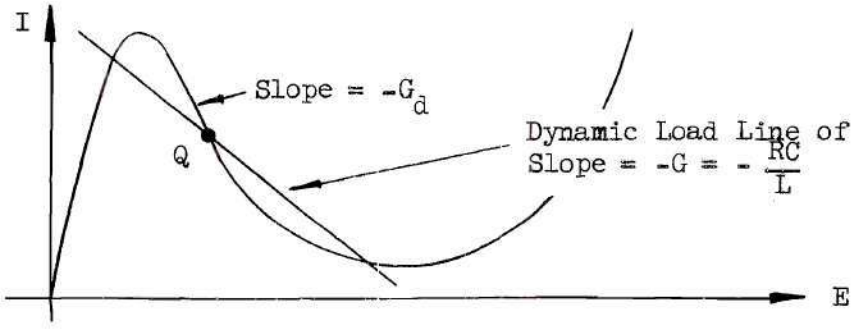

Figure 12. Dynamic Load Line Conducive to Growing Oscillations.

For condition (31) to be satisfied, it must be true that

$$\frac{4C}{L} \geq (G - G_d)^2 \quad . \tag{33}$$

The extreme values of G_d which satisfy (33) are given by

$$G_d = G \pm 2\sqrt{\frac{C}{L}} \quad . \tag{34}$$

The characteristics of the solution as a function of the circuit parameters are shown in Figure 13. The case of interest is confined to the band where near-sinusoidal oscillations are present.

The line $G_d = G$ in Figure 13 corresponds to the threshold of oscillation. For $G_d = G$, the dynamic load line is exactly tangent to the diode characteristic at the Q point.

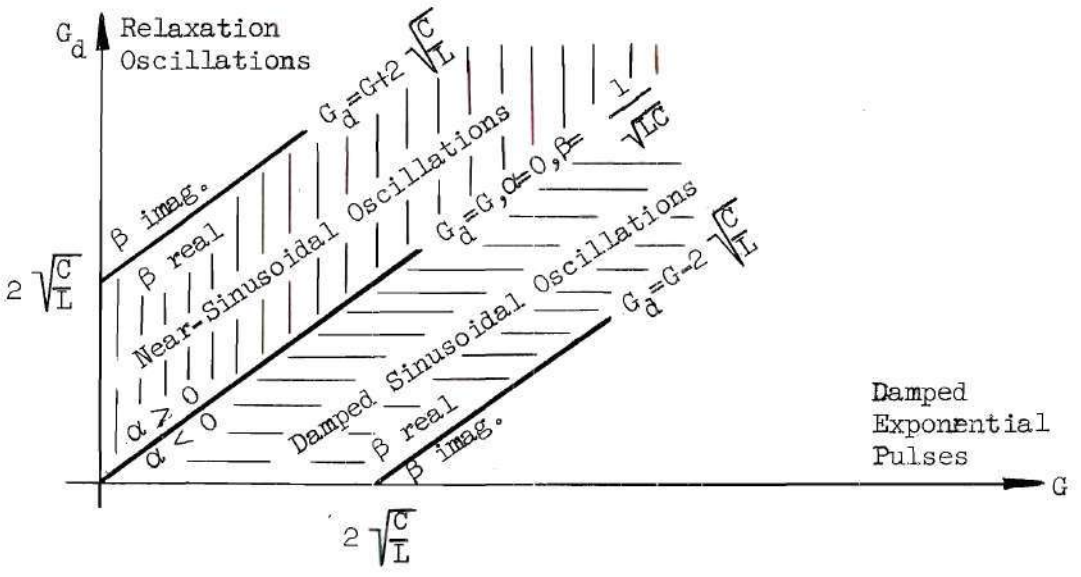

Figure 13. Influence of Circuit Parameters on the Modes of Circuit Operation. (After Strauss.)

The region corresponding to near-sinusoidal oscillations is defined in terms of the circuit parameters by

$$G \leqq G_d \leqq G + 2\sqrt{\frac{C}{L}} \quad . \tag{35}$$

Rewriting this inequality in terms of the original circuit parameters yields,

$$\frac{RC}{L} \leqq G_d \leqq \frac{RC}{L} + 2\sqrt{\frac{C}{L}} \quad . \tag{36}$$

This expression, together with the interpretation of the dynamic load line, will be useful when the effect of the circuit parameters on the near-sinusoidal behavior are discussed in a later section.

Nonlinear Analysis

Nonlinear Considerations

The linear analysis of the preceding sections is useful in gaining a preliminary understanding of the oscillator, but because it is a linear analysis of a nonlinear phenomenon it cannot be taken as a true description of the circuit behavior.

In both preceding sections, the negative dynamic resistance of the diode was considered as linear and constant. The static characteristic, shown in Figure 1(c), shows that the negative resistance is not constant and varies nonlinearly with the instantaneous voltage swing about the bias point. This fact dictates that a realistic analysis must proceed on a nonlinear basis.

A linear negative resistance implies a source of infinite power which is unrealizable in a practical circuit. The solution of equation (18) implies that if the negative resistance and circuit parameters combine in such a manner as to make α always negative the output would grow indefinitely with time. This situation is an absurdity arising from the linear analysis of a nonlinear phenomenon. Actually, all devices which display negative dynamic resistance must have an E-I characteristic which displays a positive slope on each side of the region of negative slope. This fact removes the absurdity of infinite amplitude at the output because the increasing voltage swing about the bias point will eventually pass into the dissipative regions of the characteristic during some portion of its cycle, and the energy lost there will limit the final amplitude of oscillation. In a linear system, the amplitude of oscillation, as denoted by A in equation (21), is fixed by the initial

conditions imposed on the system. In a nonlinear system of the type considered here, the initial conditions have no effect on the final amplitude of oscillation. Rather, the final amplitude is a direct consequence of the physical limitations of the device used to produce the negative resistance.

The derivation of the nonlinear differential equation which describes the oscillator begins with the basic equivalent circuit of Figure 8 which is again repeated for convenience in Figure 14. Here, the instantaneous current in the negative resistance is given by $i_\rho = f(e)$, where $f(e)$ is a nonlinear function. As before, the voltage e is the instantaneous variation from the bias point and i_ρ is the instantaneous variation of the current with respect to the bias point.

The node equation for the circuit is

$$\begin{aligned} i_L &= - i_c - i_\rho \\ &= - C \frac{de}{dt} - f(e) \ . \end{aligned} \tag{37}$$

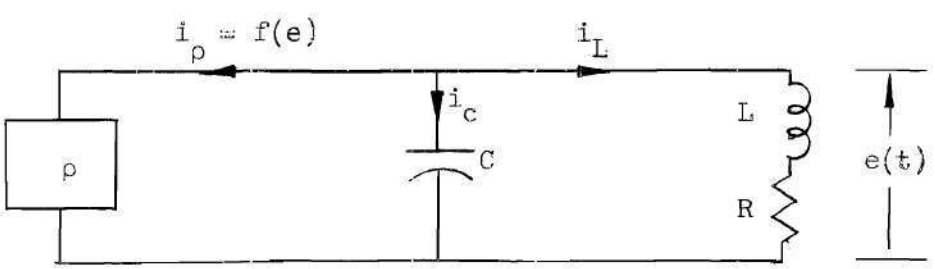

Figure 14. Basic Oscillator Circuit.

The output voltage is

$$e(t) = L \frac{di_L}{dt} + R\, i_L \ . \tag{38}$$

Substitution of equation (37) in equation (38) results in the nonlinear equation which describes the oscillator,

$$\frac{d^2e}{dt^2} + \frac{R}{L}\frac{de}{dt} + \frac{1}{LC}e + \frac{1}{C}\frac{d}{dt}\left[f(e)\right] + \frac{R}{LC}\left[f(e)\right] = 0 . \qquad (39)$$

Under the assumption of negligible series resistance, the nonlinear function f(e) is represented by the characteristic of the diode when the origin of coordinates is placed at the bias point. This graphical representation of f(e) is shown in Figure 15.

It is at this point that the lack of an analytical expression for f(e) rules out an analytical solution of the equation. As is often the case with nonlinear differential equations, the solution can be pursued on a graphical basis.

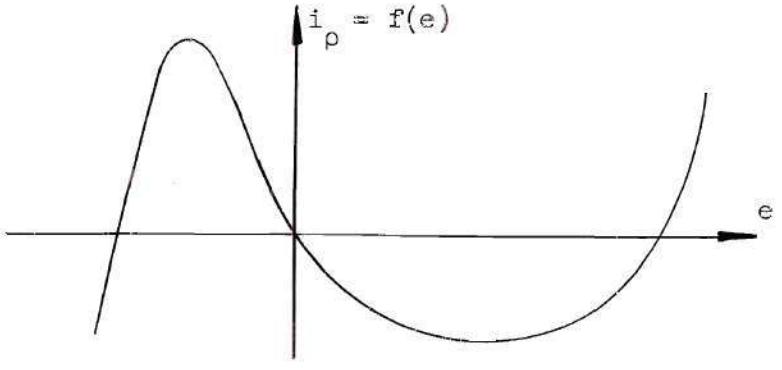

Figure 15. Diode Characteristic Used to Represent the Nonlinear Function f(e).

Graphical Solution: Method of Isoclines and Phase-Plane Analysis

Phase-plane analysis is concerned with the graphical solution of the differential equation of the form

$$\ddot{x} + A(x, \dot{x})\dot{x} + B(x, \dot{x})x = 0 , \qquad (40)$$

where the coefficients $A(x, \dot{x})$ and $B(x, \dot{x})$ are functions of the variable, x, and its time derivative, $\dot{x}$. The $x - \dot{x}$ plane is called the phase-plane, and the plot of $\dot{x}$ as a function of x describes the variations of these quantities with time.

Excellent detailed discussions of phase-plane analysis are given by Strauss (7), Truxal (8), and Cunningham (9), and only the basic fundamentals of this analysis are presented here.

The initial conditions imposed on equation (40), x(o) and $\dot{x}(o)$, fix a point on the phase-plane, and the behavior of the path from this point describes the behavior of the variables x and $\dot{x}$ for all later time. A system which is unstable is described by a path which tends to infinity, while a system which comes to rest is characterized by a path which approaches some fixed point in the phase-plane. A system which falls into a periodic oscillation is described by a path from the initial condition point which eventually traces out the same pattern with each oscillation. This closed pattern, which is reached with the steady-state, is called a limit cycle and contains much information with regard to the amplitude, frequency, and wave-shape of the oscillation. The path from the initial condition point to the limit cycle describes the transient of the solution. The method of phase-plane analysis is very useful since it yields both the transient and steady-state solutions.

The construction of a solution curve, or trajectory, in the phase-plane for equation (40) is an application of the basic graphical solution for first order equations known as the Method of Isoclines. The method of isoclines applies to equations of the form

$$\frac{dx}{dt} = \dot{x} = f(x, t) , \qquad (41)$$

and yields the solution in the form of a curve in the x-t plane.

The solution-curve is constructed by assigning numerical values to the parameters which appear in $f(x, t)$. For any point in the x-t plane, e.g. (x_1, t_1), the value of dx/dt may be numerically calculated. This value of dx/dt is then interpreted as the slope of the solution-curve through the point (x_1, t_1). At the given point (x_1, t_1) a short line segment is drawn with the calculated slope $(\frac{dx}{dt})_1$. The solution curve through that point then contains this short line segment.

The method of isoclines systematizes the construction of these short line segments by first assigning a particular numerical value for the slope. If the value chosen for the slope is m, then equation (41) becomes

$$\frac{dx}{dt} = \dot{x} = f(x, t) = m , \qquad (42)$$

and is then an equation of the locus of all points in the x-t plane through which pass solution-curves with slope equal to m. Using equation (42) this locus, called an isocline, may be constructed. After construction of the isocline, short line segments are drawn all along it with each line segment having a slope m. The process is then repeated by picking new values of m and constructing new isoclines until the x-t plane is filled with isoclines, each carrying a number of short line segments of appropriate slope.

The initial condition imposed on the equation, e.g. (x_o, t_o), then determines the solution-curve in the x-t plane. Starting from the initial point, the solution-curve is traced out by following the slope of the directed line segments which fill the plane. Since equation (42)

requires that the slope given by f(x, t) be single-valued at all points other than singularities of the equation, it follows that no two solution curves can cross through the same point in the x-t plane. Therefore, for each initial condition imposed on the system described by equation (41), there will be a single, unique solution-curve.

The results of a construction by the isocline method for an arbitrary equation (41) are shown in Figure 16. In a practical solution many more isoclines than shown in Figure 16 would be necessary for good accuracy.

In order to apply the method of isoclines to equation (39), it must be reduced to an equation of the first order. This is done by introducing the new variables

$$\tau \triangleq \omega_o t \ , \tag{43}$$

where

$$\omega_o \triangleq \frac{1}{\sqrt{LC}} \ , \tag{44}$$

and

$$\nu \triangleq \frac{de}{d\tau} = \frac{1}{\omega_o} \frac{de}{dt} \ . \tag{45}$$

The derivatives now become

$$\frac{de}{dt} = \left(\frac{de}{d\tau}\right)\left(\frac{d\tau}{dt}\right) = \omega_o \nu \ , \tag{46}$$

and

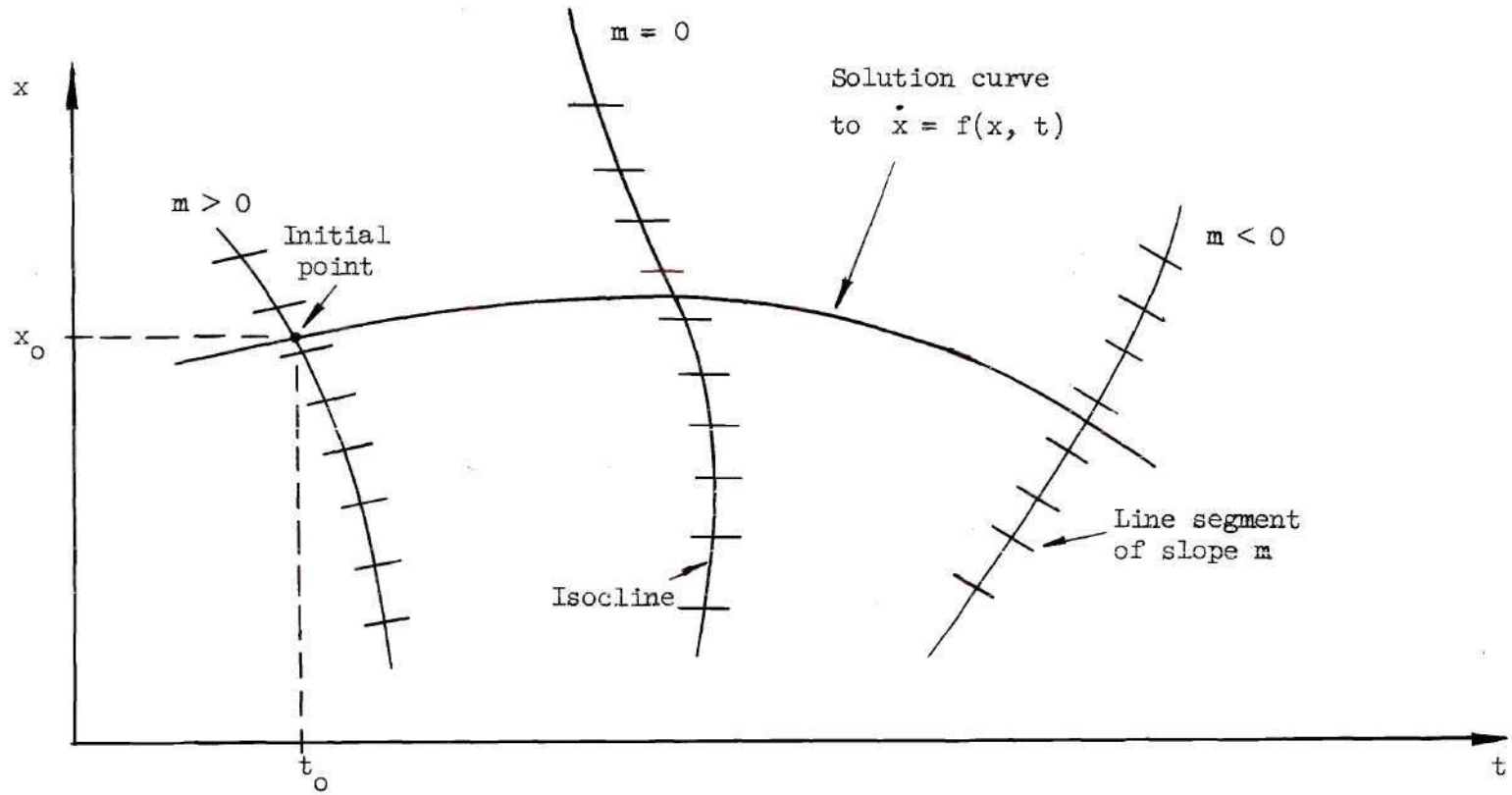

Figure 16. Simplified Construction of Arbitrary Solution Curve Using the Method of Isoclines.

$$\frac{d^2e}{dt^2} = \left(\frac{d^2e}{d\tau^2}\right)\left(\frac{d\tau}{dt}\right)^2 + \left(\frac{de}{d\tau}\right)\left(\frac{d^2\tau}{dt^2}\right) = \omega_o^2\, \nu \left(\frac{d\nu}{de}\right) . \qquad (47)$$

The substitution of equations (44), (46), and (47), in equation (39) yields the simpler equation

$$\omega_o^2\, \nu\left(\frac{d\nu}{de}\right) + \frac{R}{L}\,\omega_o \nu + \omega_o^2\, e + \frac{1}{C}\frac{d}{dt}\left[f(e)\right] + R\,\omega_o^2\left[f(e)\right] = 0. \qquad (48)$$

Equation (48) is a first-order equation of the same form as equation (41). The variables are now $(d\nu/de)$, ν, and e, and the solution-curve is the trajectory in the ν-e plane.

The introduction of the new variable ν normalizes the phase-plane so that if the variable e is a perfect sinusoid, e.g. A sin $\omega_o t$, then ν = A cos $\omega_o t$, and the trajectory in the normalized phase-plane will have a limit cycle which is a perfect circle of radius A.

In equation (48), the presence of the time derivative of the function f(e) makes it impossible to compute the location of the isoclines in the ν-e plane by direct numerical substitution. At this point, it is desirable to make the change of variable

$$\frac{df}{dt} = \left(\frac{df}{de}\right)\left(\frac{de}{dt}\right) = \omega_o \nu \left(\frac{df}{de}\right) . \qquad (49)$$

With the substitution of equation (49), equation (48) may be rewritten so that the isoclines may be computed as

$$\nu = \frac{-e - R\left[f(e)\right]}{\left(\frac{d\nu}{de}\right) + R\sqrt{\frac{C}{L}} + \sqrt{\frac{L}{C}}\left(\frac{df}{de}\right)} . \qquad (50)$$

The isoclines are computed, as before, by choosing a value m for the slope of the phase-trajectory (dv/de), and computing the points (v, e) which define the isocline for that slope. The value of f(e) for various values of e may be read from the graphical representation of f(e) as shown in Figure 17(a). The value of (df/de) for the various values of e may be taken from a curve for (df/de) which has been graphically constructed from the curve for f(e). This is shown in Figure 17(b).

Using equation (50) and curves as shown in Figure 17, the phase-plane may be filled with isoclines corresponding to different values of m assigned to (dv/de). The introduction of the dimensionless time variable τ makes the dimensions of v and e the same. If equal numerical scales are chosen on the v and e axes, then the value m assigned to (dv/de) is the actual geometrical slope to be plotted for the directed line segments on the isoclines (10). A simple example of the construction of a phase trajectory corresponding to a periodic oscillation is shown in Figure 18.

Since time is an implicit parameter in the phase-portrait, the instantaneous voltage as a function of time must also be constructed graphically. One method for finding the time required for the system to change from one state to another (e.g., point 1 to point 2 in Figure 18) is to consider the original definition

$$v = \frac{de}{d\tau} = \frac{1}{\omega_o} \frac{de}{dt} . \qquad (51)$$

Therefore

$$dt = \frac{1}{\omega_o} \frac{1}{v} de . \qquad (52)$$

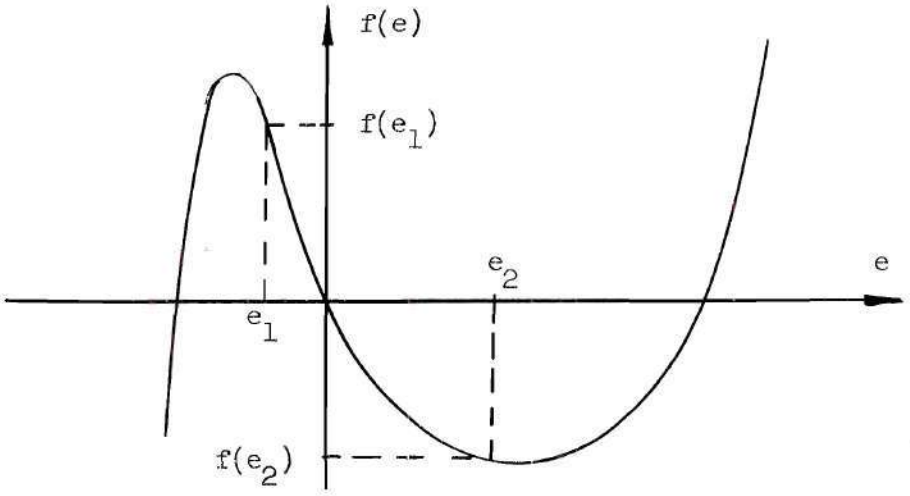

Figure 17(a). Numerical Evaluation of f(e) for Use in Equation (50).

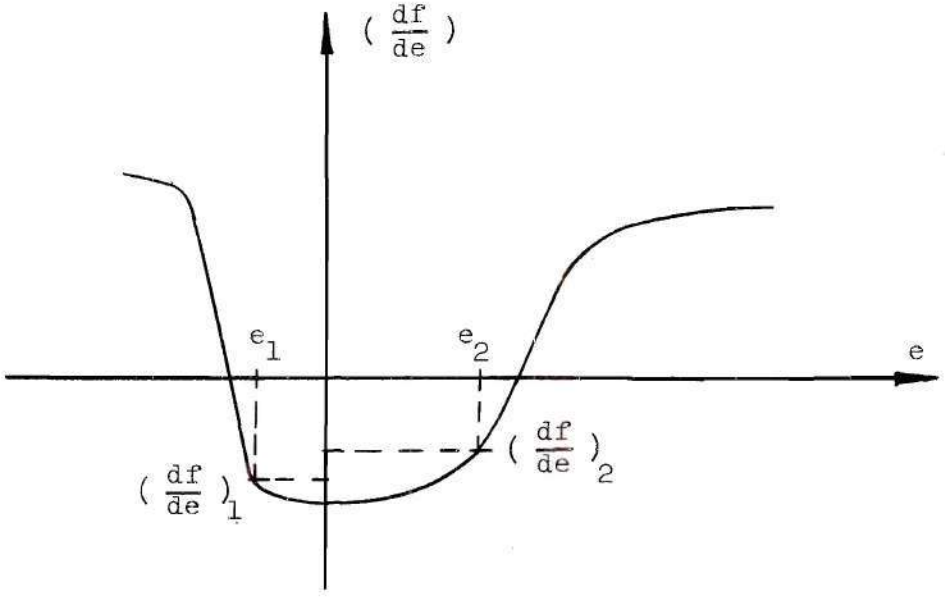

Figure 17(b). Numerical Use of the Graphical Construction for $\left(\frac{df}{de}\right)$.

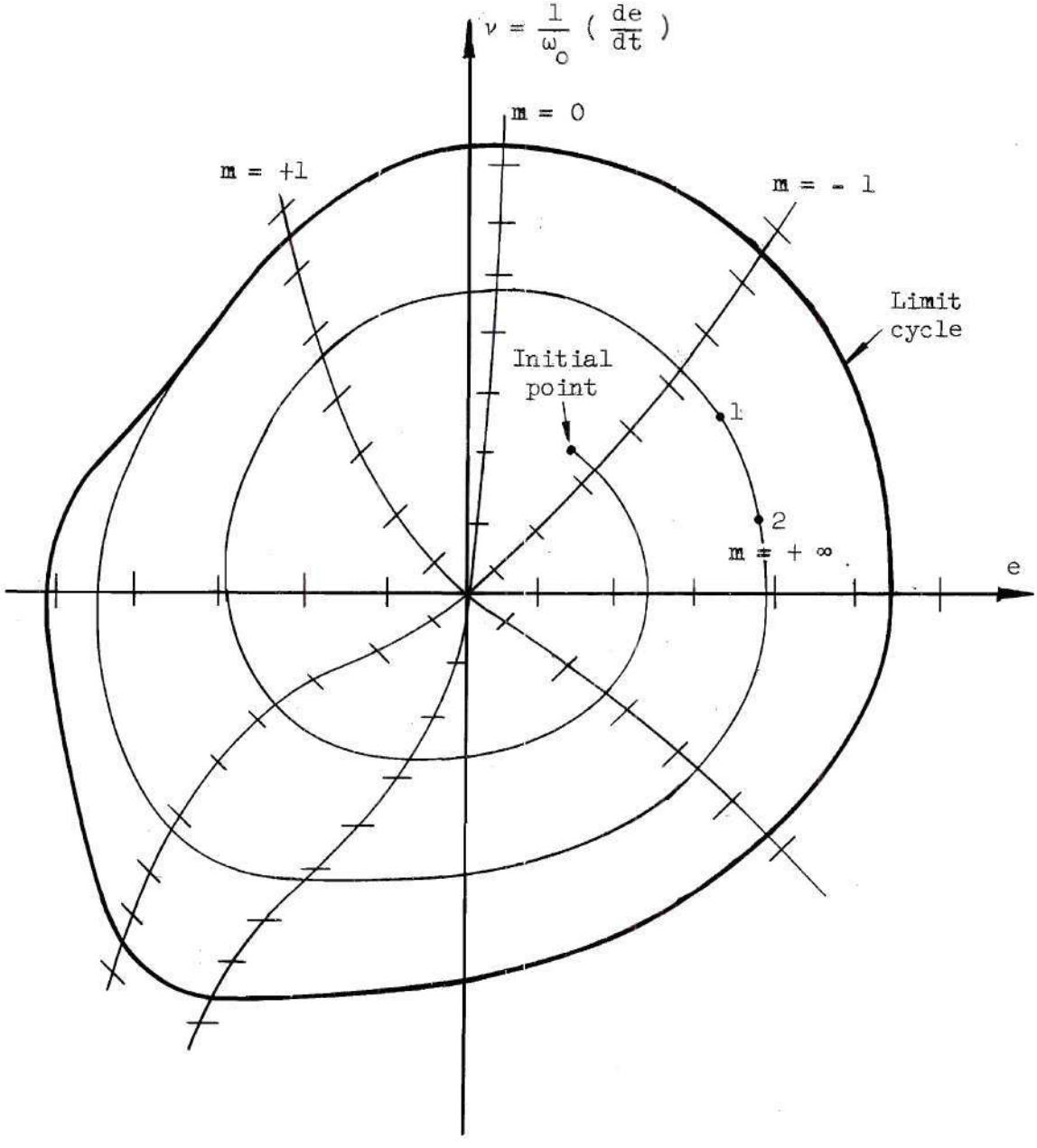

Figure 18. Example of a Phase Trajectory.

The time required for the instantaneous voltage to change from e_1 to e_2 (corresponding to points 1 and 2 in Figure 18) is then given by

$$t_{1\text{-}2} = \frac{1}{\omega_o} \int_{e_1}^{e_2} \frac{1}{\nu} \, de \, . \qquad (53)$$

The integrand $\frac{1}{\nu}$ is plotted as a function of e, and the integral is given by the area under the curve between the limits of e_1 and e_2. The procedure is then repeated and the construction continued until the desired portion of the instantaneous waveshape is obtained.

CHAPTER III

INSTRUMENTATION AND PROCEDURE

Approach to the Problem

Method of Solution

An accurate solution of any nonlinear differential equation by numerical phase-plane analysis is, at best, a laborious procedure. For this reason, a solution is sometimes obtained with an analog computer. This method is especially convenient since the computer can usually be programmed to plot the phase-plane trajectories and the time-varying waveform simultaneously. A unique feature of the computer solution is that the time required to make changes in the program corresponding to changes in the circuit parameters of the oscillator is negligible when compared to the time required to manually reconstruct the phase-plane trajectories and time-varying waveforms. The computer can thus be used to determine the role of each parameter in the total solution for the output waveshape of the oscillator.

Because the computer is more accurate than a manual solution, and new solutions are obtained in a comparatively short time, this approach to the problem was used.

Function Generator

The first problem in programming equation (39) on the analog computer is the construction of a nonlinear function generator which will represent the function f(e). A basic circuit which illustrates the principle of the function generator is shown in Figure 19. The voltage

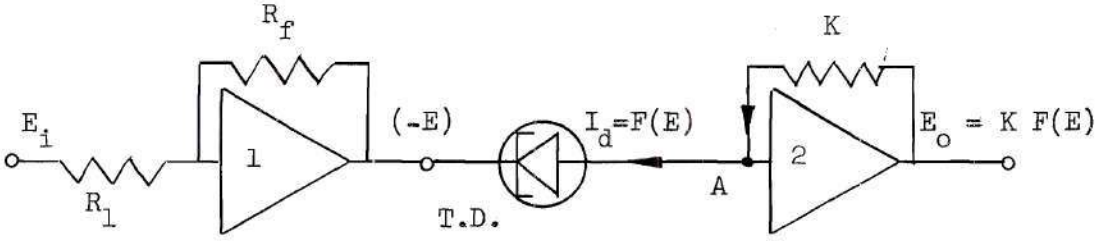

Figure 19. Basic Function Generator.

E_i is reduced to the proper level by amplifier 1, and since point A is held at virtual ground by the high gain of operational amplifier 2, the voltage E appears across the tunnel diode. The diode will then draw a current $I_d = F(E)$ which produces an output from amplifier 2 proportional to the diode characteristic F(E).

Because of the inherent instability of the tunnel diode when biased in the region of negative resistance, a practical form of the function generator requires that the tunnel diode be stabilized by shunting it with a resistance. The value of the resistance to be used must be found by considering the equivalent circuit of the parallel combination of the diode and resistor shown in Figure 20. The driving point impedance, Z(s), is

$$Z(s) = \frac{R_p\left[s^2 + \left(\frac{R_s}{L_s} - \frac{G_d}{C_d}\right)s + \left(\frac{1 - R_s G_d}{L_s C_d}\right)\right]}{s^2 + \left(\frac{R_s + R_p}{L_s} - \frac{G_d}{C_d}\right)s + \frac{1 - (R_s + R_p)G_d}{L_s C_d}} . \qquad (54)$$

If the network is to be non-oscillatory, then Z(s) must be stable which requires that all its poles and zeros fall in the left-half s-plane. This requires that R_p fall in the range corresponding to

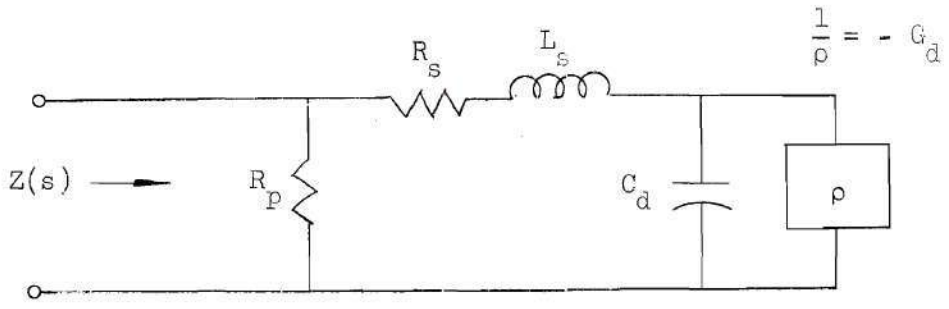

Figure 20. Equivalent Circuit of Parallel Combination.

$$L_s \frac{G_d}{C_d} < R_s + R_p . \tag{55}$$

For the diodes used, an R_p of 100 ohms is a suitable value so that the parallel combination of R_p and the diode is stable and at the same time the impedance of the combination is high enough to avoid excessive current drain from the operational amplifier. The resistance R_p must be mounted as close as is physically possible to the diode in order to keep the parasitic circuit parameters at a minimum. After the addition of R_p, a stabilized E-I characteristic is obtained as shown in Figure 21.

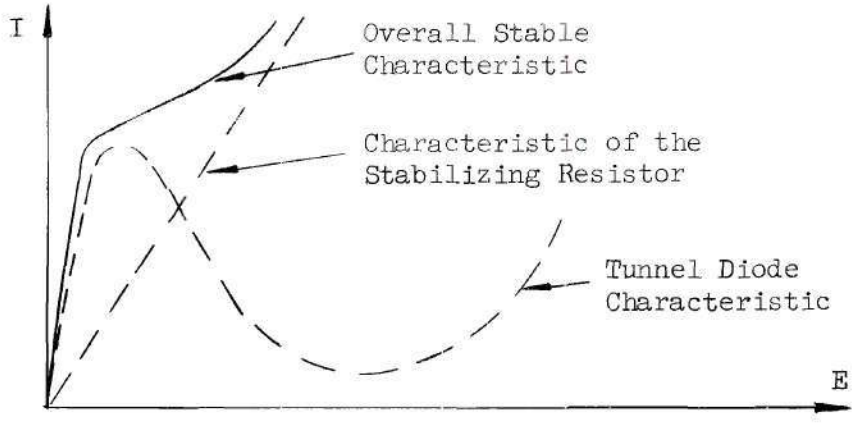

Figure 21. Stabilized E-I Characteristic of the Parallel Combination.

An output which is proportional to the actual diode characteristic F(E) is then obtained by subtracting the characteristic of the stabilizing resistor from the overall characteristic of Figure 21.

The resulting function generator is shown in Figure 22, and its operation may be described as follows: Since point A is held at virtual ground, the voltage E appears across the parallel combination of the 100 Ω resistor and the tunnel diode. The current drawn by the combination consists of the diode current, F(E), and the current in the resistor, $\left(\frac{E}{100} \right)$. Assuming ideal operational amplifiers, this total current flows through the 5000 ohm feedback resistance around amplifier 2 so that the output voltage of that amplifier is

$$E_2 = 5000 \left[F(E) + \frac{E}{100} \right] . \qquad (56)$$

The voltage E_2 is then fed to the sign-changer of amplifier 3 so that its output is

$$E_3 = - 5000 \left[F(E) + \frac{E}{100} \right] . \qquad (57)$$

By inspection, the output of amplifier 4 is

$$E_4 = 5000 \left[\frac{E}{100} \right] . \qquad (58)$$

The voltages E_3 and E_4 are then fed to the summing amplifier 5 whose output is

$$\begin{aligned} E_o &= - (E_3 + E_4) \\ &= - \left[- 5000\ F(E) - 50E + 50E \right] . \end{aligned} \qquad (59)$$

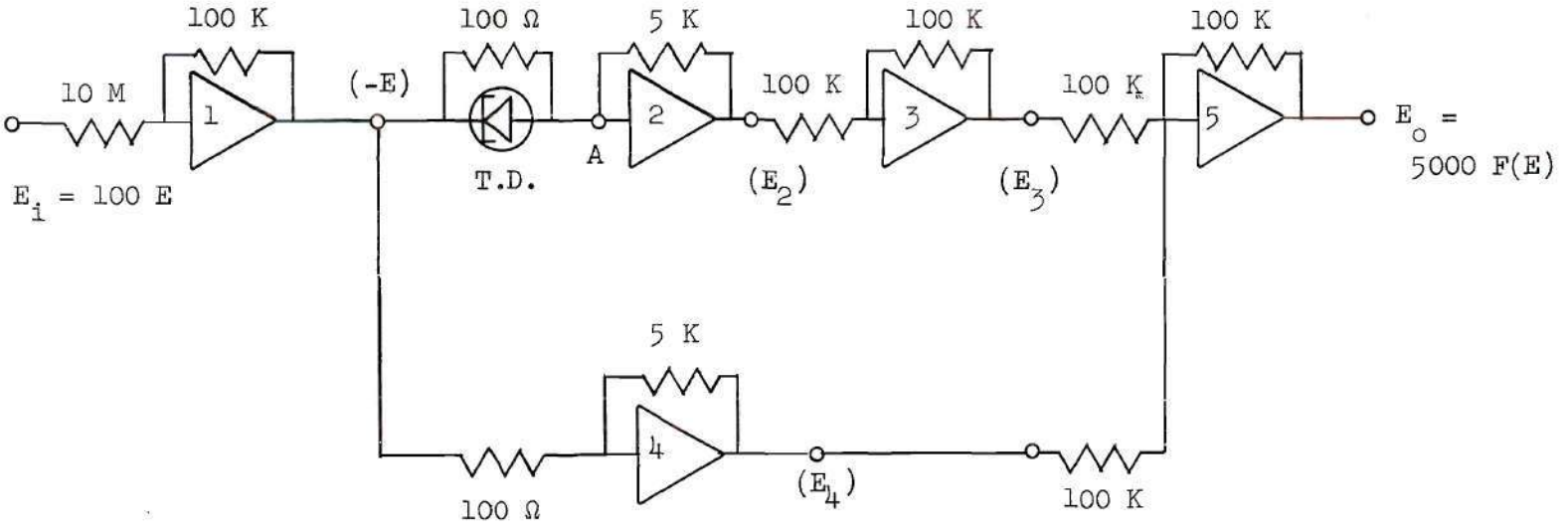

Figure 22. Modified Function Generator.

Therefore, the output of the circuit is

$$E_o = 5000\ F(E)\ , \qquad (60)$$

which is the desired result.

The feedback resistance around amplifiers 2 and 4 was chosen so that the effective gain of 2 and 4 is not so high that small disturbances will cause these amplifiers to saturate. The overall circuit may then be calibrated by replacing the tunnel diode by a precision resistor. Since the output is 5000 F(E), and the 1N2940 diode has a typical peak current of 1 ma over the range of interest, the circuit produces a peak output of 5 volts. An example of the function generator output is shown in Figure 23.

The circuit of Figure 22 is actually not a function generator in the true sense of the phrase. Rather, it is a characteristic generator since it gives the characteristic of the diode with respect to the true origin. The function generator required is one which produces an output as shown in Figure 15. The origin of the coordinates must be movable and the output must be zero at that point.

The circuit of Figure 22 is easily modified so that it is a true function generator. Consider the situation depicted by Figure 24. The origin of the function f(e) is to be fixed at the bias voltage E_1. At this point the quiescent current is I_1, and the output of the characteristic generator is then 5000 I_1 volts. The circuit of Figure 22 may be modified by adding an additional DC input to amplifier 1 so that any bias voltage E_1 may be chosen for the coordinates. The DC output voltage, 5000 I_1, is then eliminated by feeding a DC voltage of the proper magnitude

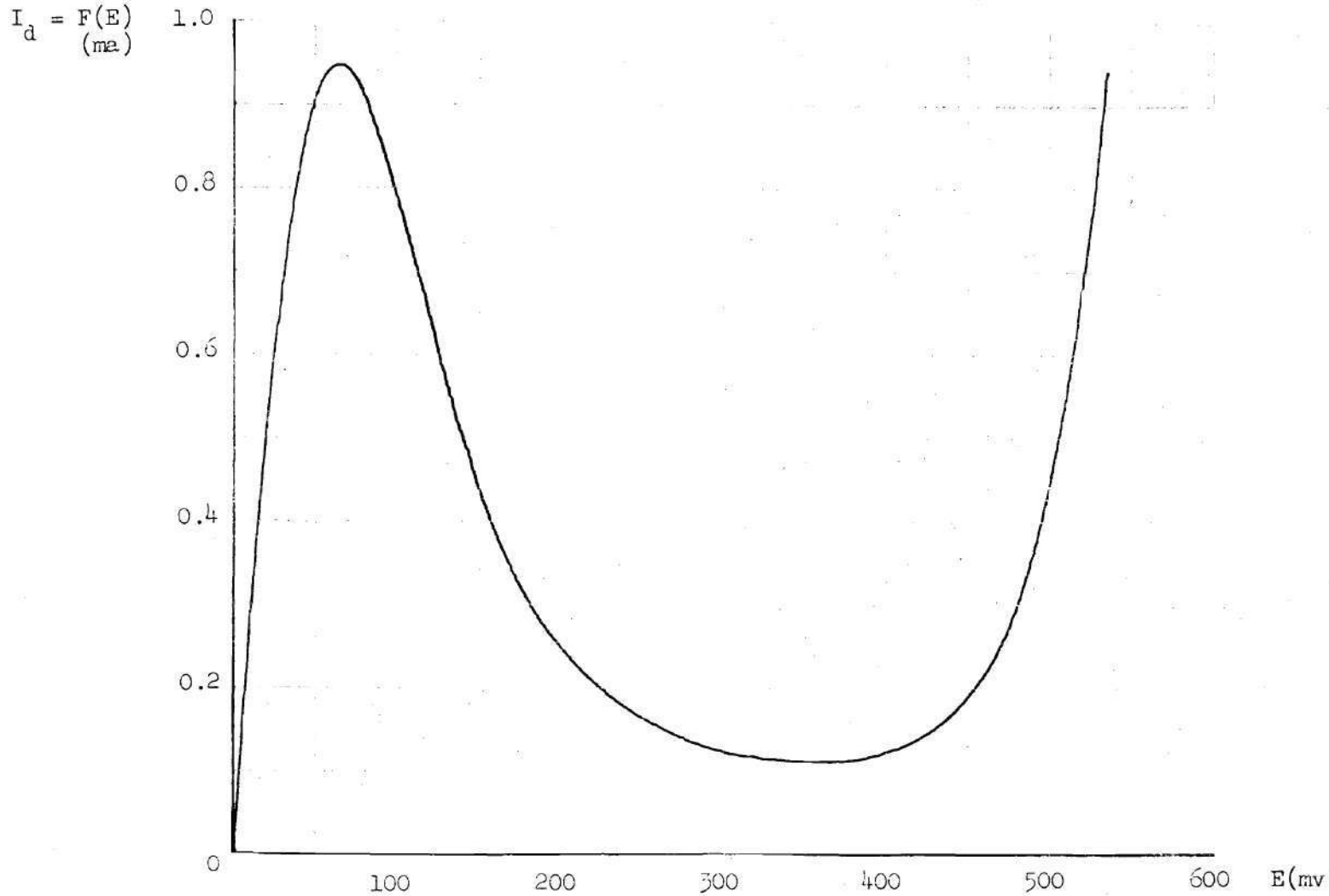

Figure 23. Output of the Function Generator.

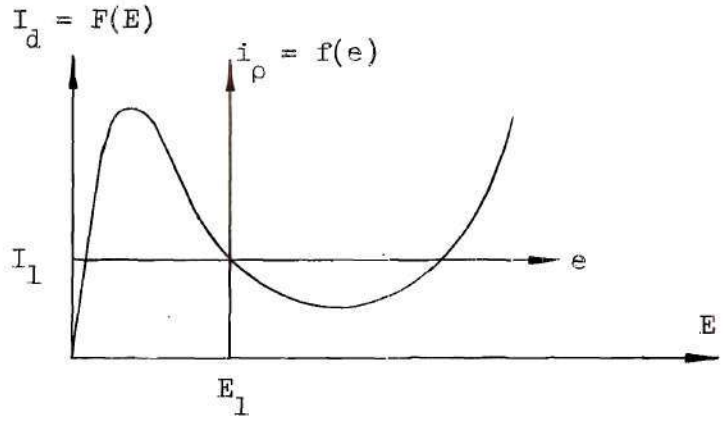

Figure 24. Derivation of the Function f(e).

and polarity to the input of the summing amplifier 5 so as to cancel the signal at the output.

The true function generator is shown in Figure 25, and its output is proportional to the true f(e) of Figure 15. The origin of f(e) may be chosen at any point on the diode characteristic, and the output may be adjusted to zero at that point.

Computer Solution

Final Machine Equation

The final machine equation is obtained by integrating equation (39) which yields

$$\frac{de}{dt} + \frac{R}{L} e + \frac{1}{LC} \int e \, dt + \frac{1}{C} f(e) + \frac{R}{LC} \int f(e) \, dt = 0 . \qquad (61)$$

The unscaled block diagram of the computer solution to equation (61) is shown in Figure 26. The details of the scaled program are contained in Appendix B.

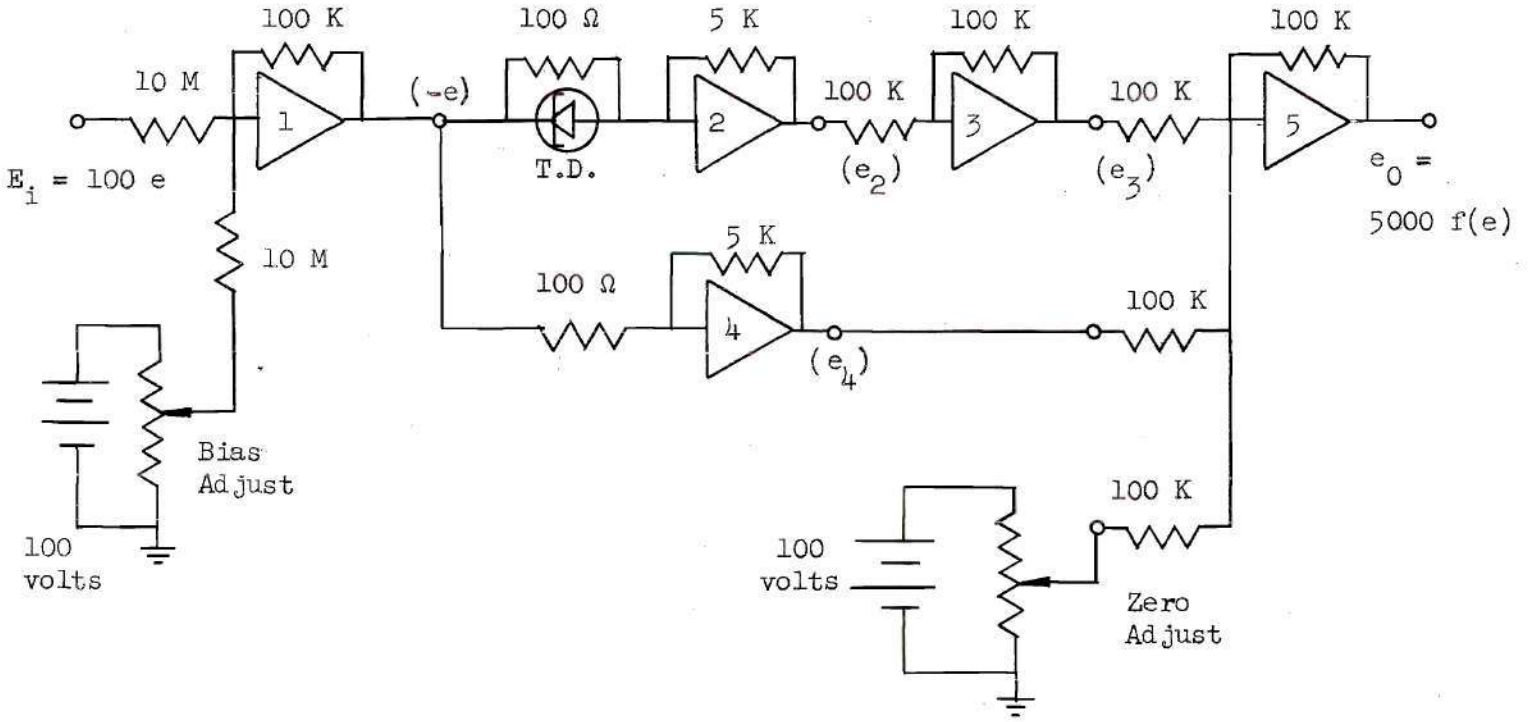

Figure 25. True Function Generator.

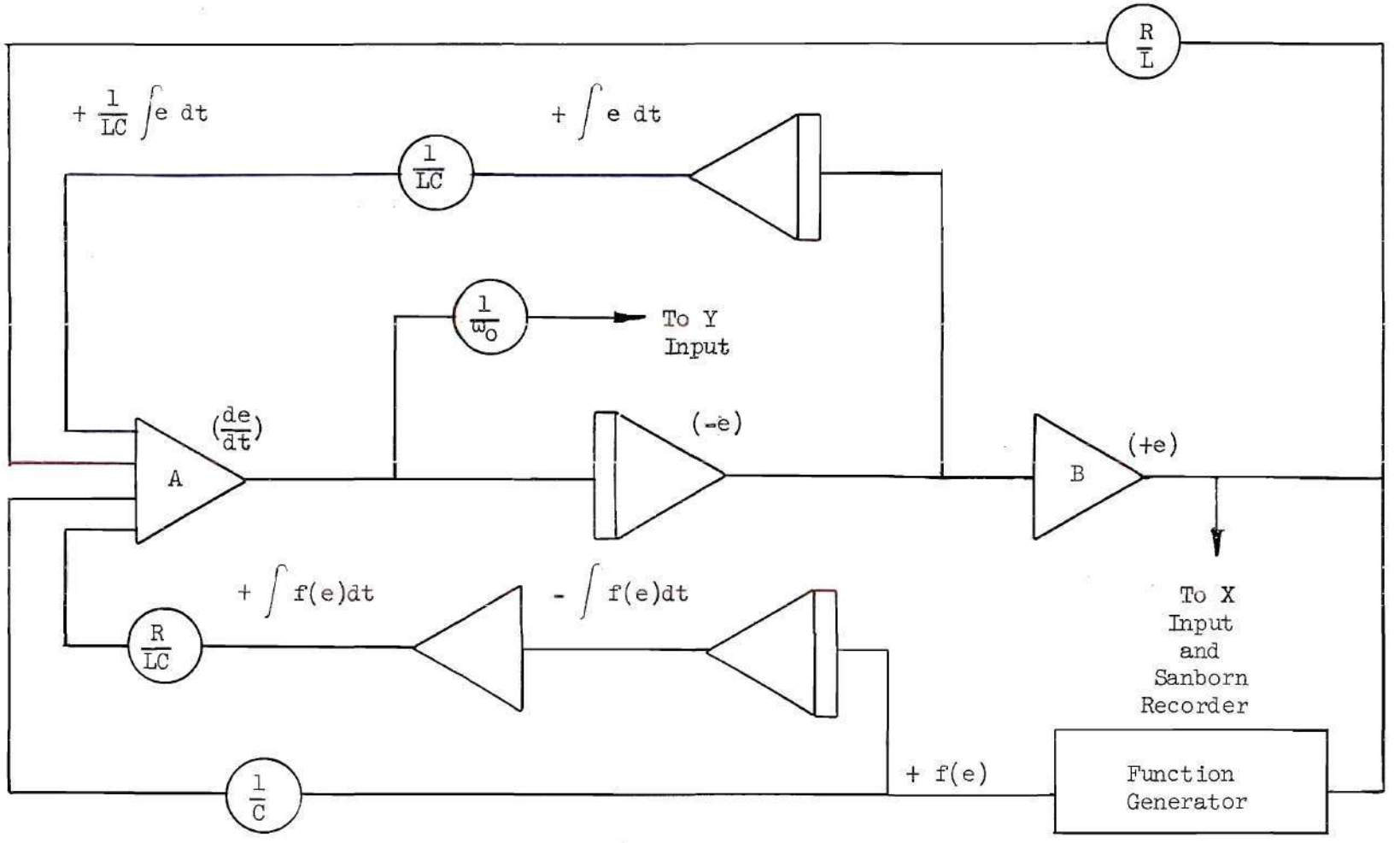

Figure 26. Unscaled Computer Solution of Equation (61).

Method of Recording Computer Data

The outputs of amplifiers A and B of Figure 26 were used to drive a Moseley Autograph X-Y Recorder which traced out the phase-plane trajectory from the initial condition to the limit cycle. The output of amplifier B was also fed to one channel of a Sanborn Recorder which traced out the time-varying waveform simultaneously. An example of the computer solution recorded in this manner is shown in Figure 27.

Definition of Circuit Parameters

The circuit parameters which were varied are now defined in terms of the parameters of the tank circuit shown in Figure 28.

In the sinusoidal-steady-state, the impedance of the tank circuit at resonance is

$$Z = \frac{1}{R}\left(\frac{L}{C}\right) . \tag{62}$$

At this point, it is useful to assign base values to the parameters of equation (62) so that

$$Z_b \triangleq \frac{1}{R_b}\left(\frac{L_b}{C_b}\right) , \tag{63}$$

where the subscript b indicates base values. The impedance level of the circuit for all further analysis is now defined in terms of the ratio L_b/C_b. If the substitutions

$$L = K_z L_b , \tag{64}$$

$$C = C_b/K_z , \tag{65}$$

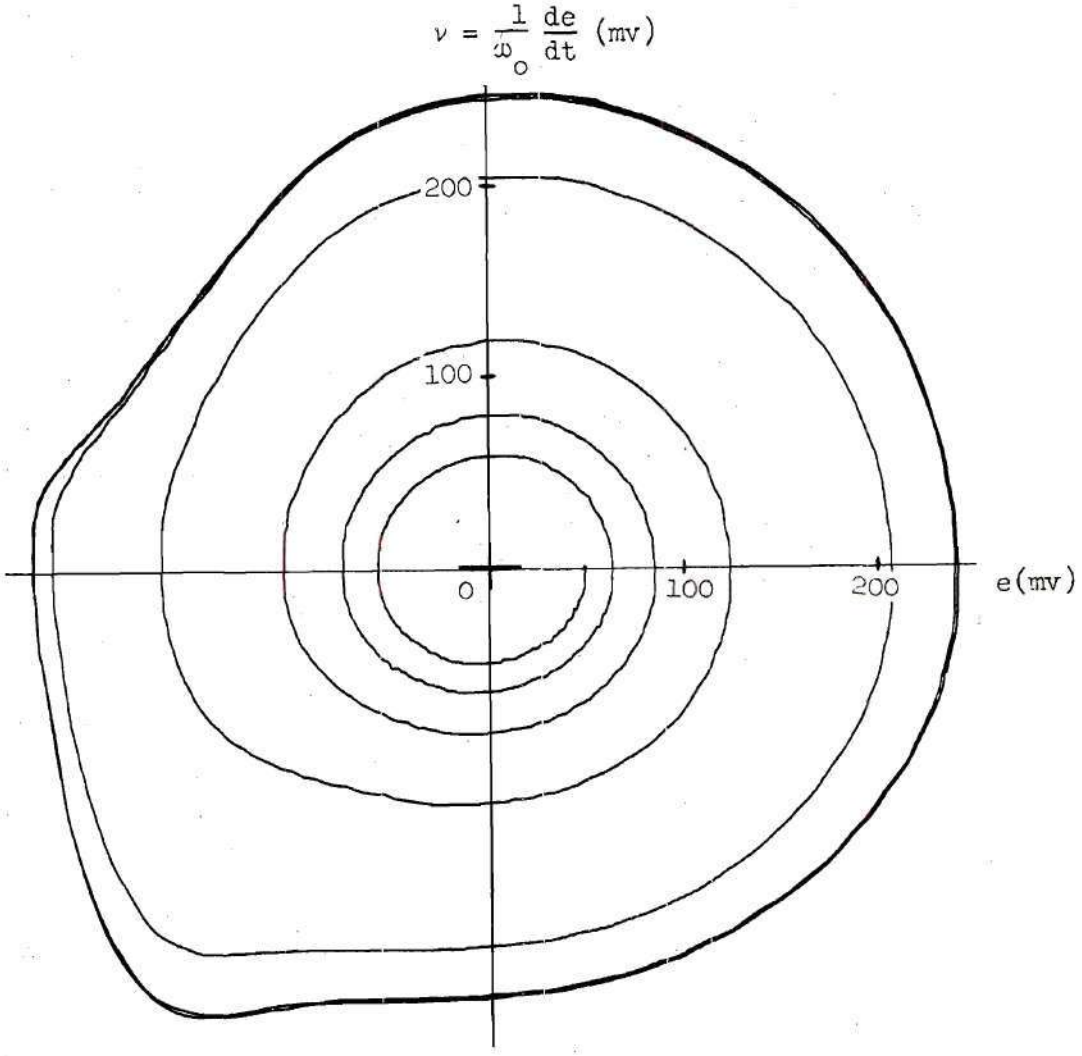

Figure 27(a). Computer Solution for the Phase Trajectory.

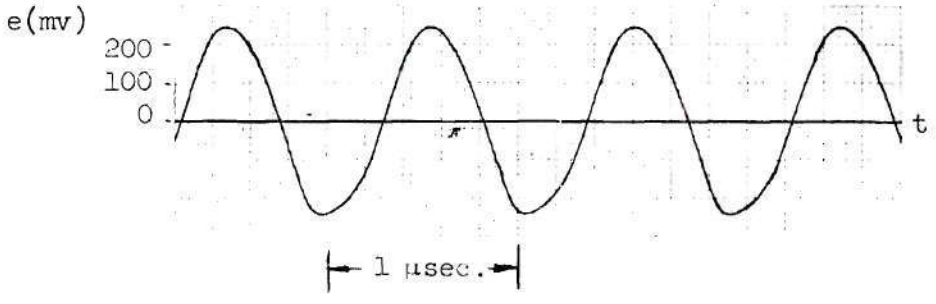

Figure 27(b). Computer Solution for the Instantaneous Waveform.

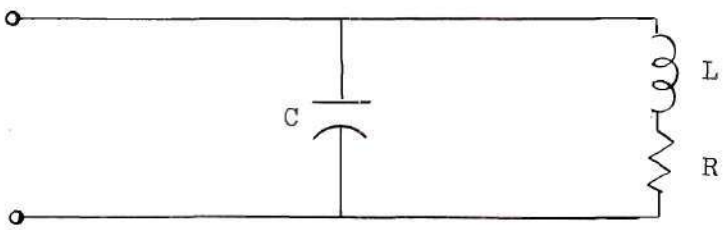

Figure 28. Tank Circuit.

and

$$R = R_b \ , \tag{66}$$

are made in equation (62), then the impedance may be written in general as

$$Z = \frac{1}{R_b} \left(K_z^2 \frac{L_b}{C_b}\right) = K_z^2 \left(\frac{L_b}{R_b C_b}\right) = K_z^2 \left(Z_b\right) \ . \tag{67}$$

The definition of equation (67) is useful since the value of the dimensionless factor K_z sets the impedance level of the circuit with respect to the base value Z_b.

For the purpose of analysis, the Q of the circuit is defined as

$$Q \triangleq \frac{\omega_o L}{R} = \frac{1}{R}\sqrt{\frac{L}{C}} \ , \tag{68}$$

where

$$\omega_o \triangleq \frac{1}{\sqrt{LC}} \ . \tag{69}$$

Again, it is useful to make use of a definition in terms of base values, so that

$$Q_b = \frac{1}{R_b}\sqrt{\frac{L_b}{C_b}} \tag{70}$$

represents the base value of the circuit Q. The parameter Q may now be written in a general form. Substitution of equations (64) and (65) in equation (68) together with the relation

$$R = K_r R_b \ , \tag{71}$$

yields

$$Q = \frac{1}{K_r R_b}\sqrt{K_z^2 \frac{L_b}{C_b}} = \frac{K_z}{K_r}\left[\frac{1}{R_b}\sqrt{\frac{L_b}{C_b}}\right] = \frac{K_z}{K_r} Q_b \ . \tag{72}$$

This general relation for Q is a useful form since it shows explicitly the effect of the impedance level on the circuit Q and at the same time allows the Q to be varied by means of the dimensionless factor K_r even though the impedance level, as defined, may be held constant.

Variation of the Circuit Parameters

Rewriting equation (61) in terms of the base values R_b, L_b, C_b and the variable factors K_z and K_r yields

$$\frac{de}{dt} + \frac{K_r R_b}{K_z L_b} e + \frac{1}{L_b C_b}\int e\, dt + \frac{K_z}{C_b} f(e) + \frac{K_r R_b}{L_b C_b}\int f(e)\, dt = 0. \tag{73}$$

Varying the impedance level and circuit Q changes some of the coefficients in equation (73) which demands that changes be made in the computer program.[2] For this reason, the impedance level and circuit Q are not

---

[2]For the details of the scaling procedure and method of changing the program, the reader is referred to Appendix B.

easily varied in a continuous manner. Since bias is changed in the function generator simply by changing the setting of a potentiometer, it may be varied smoothly. The data were taken under these conditions by picking K_z and Q (which fixes K_r) in steps and then varying the bias between the limits of oscillation.

The data were taken systematically through the use of a three-dimensional model as shown in Figure 29. In Figure 29, the impedance level has been fixed, for example, at $K_z = 2$ and K_r picked through the use of equation (72) so that $Q = 2Q_b$. The bias range over which oscillations occurred and solutions were obtained is indicated by the heavy line AB. This process was then repeated for different values of K_z and Q and data taken over the three-dimensional space shown in Figure 29.

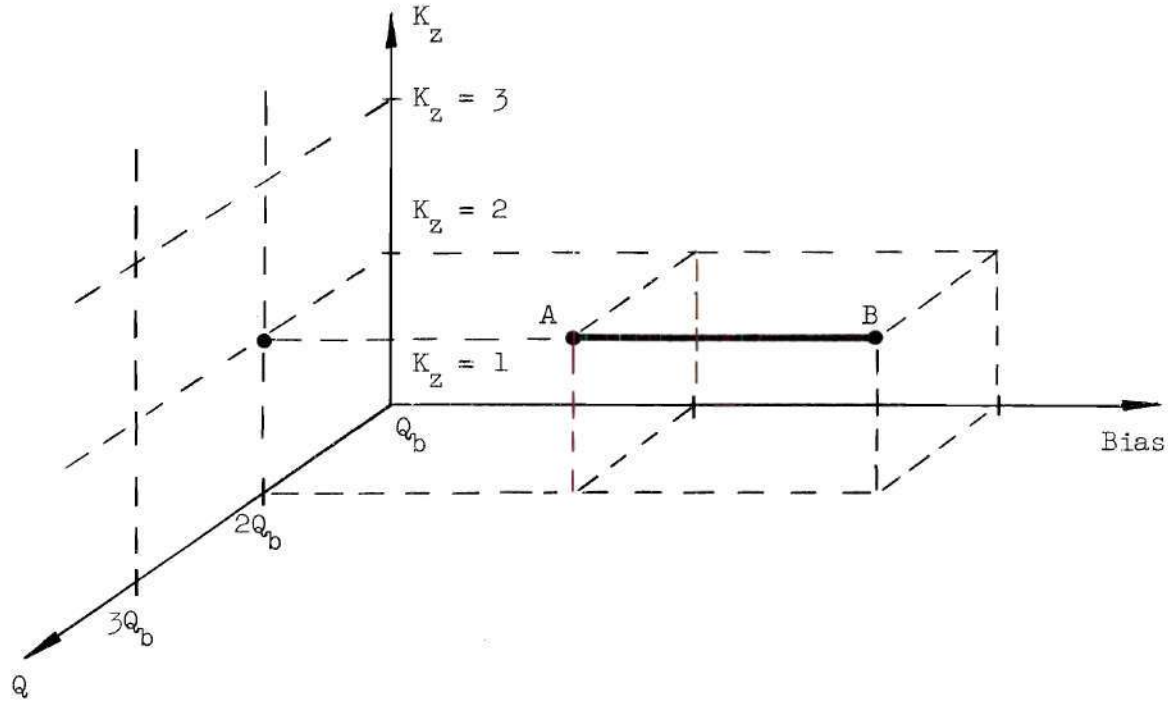

Figure 29. Three Dimensional Model Used to Systematize Taking Data.

CHAPTER IV

EXPERIMENTAL RESULTS

Near-Sinusoidal Oscillations

General Approach

In the following sections the experimental results for the near-sinusoidal mode of circuit operation are discussed from various points of view. As stated in Chapter I, the characteristic of the circuit behavior which is of greatest interest is the waveshape of the steady-state output voltage.

The objective of this chapter is to consider separately each of the circuit parameters and its influence on the output waveshape. To explain the role of each circuit parameter in the distortion of the waveshape, various heuristic techniques are used. Among these are the quasi-linear analysis presented earlier, load line techniques, and a consideration of the assymmetry of the diode characteristic. An effort is made to show the influence of each circuit parameter on the output waveshape by more than one approach. Finally, the overall effect of the circuit parameters when all three parameters are varied simultaneously is discussed from the system-root point of view.

Quasi-Linear Considerations

The results of the near-sinusoidal case can be reviewed in terms of the quasi-linear analysis given in Chapter II. In terms of the base values of the circuit parameters inequality (36), which defines near-sinusoidal operation, becomes

$$\frac{K_r}{K_z^2}\left(\frac{R_b C_b}{L_b}\right) \leq G_d \leq \frac{K_r}{K_z^2}\left(\frac{R_b C_b}{L_b}\right) + \frac{2}{K_z}\sqrt{\frac{C_b}{L_b}} \quad , \tag{74}$$

or

$$\frac{K_r}{K_z^2}(G_b) \leq G_d \leq \frac{K_r}{K_z^2}(G_b) + \frac{2}{K_z}\sqrt{\frac{C_b}{L_b}} \quad , \tag{75}$$

where G_b is the base value of the equivalent shunt conductance of the tank circuit and is expressed as

$$G_b = \frac{R_b C_b}{L_b} \quad . \tag{76}$$

The region of interest, as shown in Figure 30, is the band defined by inequality (75) where near-sinusoidal oscillations are present. From Figure 30, the allowable range of external conductance may be found. Assuming that the diode is biased in its most linear region, where $G_d = (G_d)_{max}$, the threshold of oscillation occurs at point A, where

$$G = G_{max} = (G_d)_{max} \quad . \tag{77}$$

The lowest permissible value of G occurs at point B where

$$(G_d)_{max} = G_{min} + 2\sqrt{\frac{C}{L}} \quad . \tag{78}$$

The allowable range of variation in G is then

$$\Delta G = G_{max} - G_{min} = (G_d)_{max} - \left[(G_d)_{max} - 2\sqrt{\frac{C}{L}}\right]$$
$$= 2\sqrt{\frac{C}{L}} \quad . \tag{79}$$

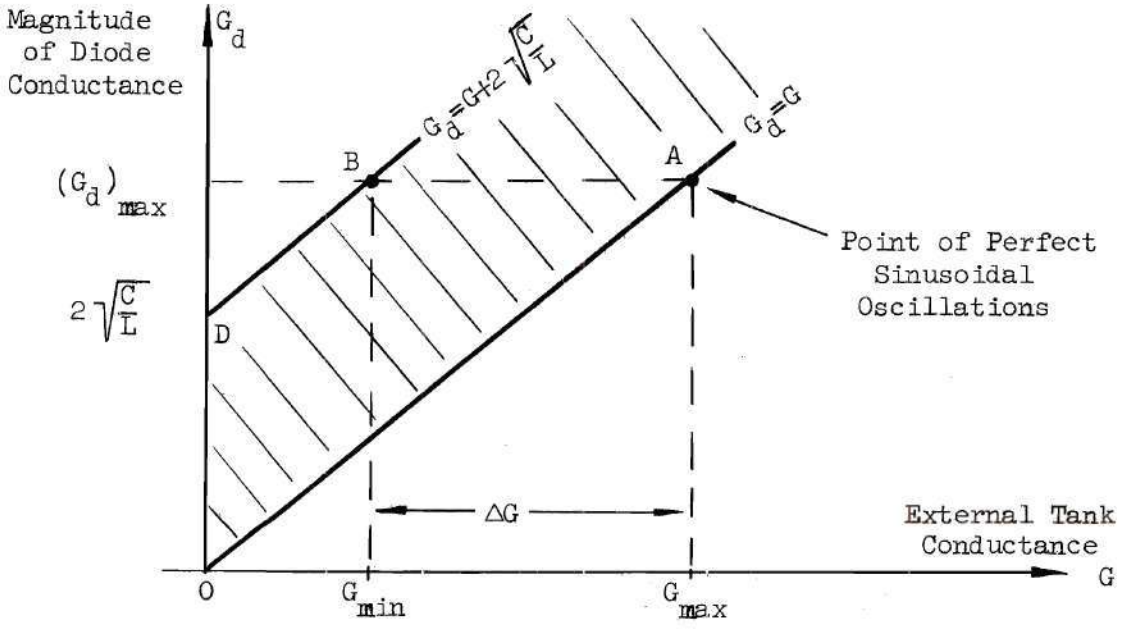

Figure 30. Allowable Range of Variation in External Tank Conductance for Near-Sinusoidal Oscillations.

In terms of base values, equation (79) becomes

$$\Delta G = \frac{2}{K_z}\sqrt{\frac{C_b}{L_b}} \quad . \tag{80}$$

The height of the band defining near-sinusoidal oscillations (the line segment $\overline{OD}$ in Figure 30) may be expressed as

$$\overline{OD} = 2\sqrt{\frac{C}{L}} = \frac{2}{K_z}\sqrt{\frac{C_b}{L_b}} \quad . \tag{81}$$

With the aid of this quasi-linear analysis, the effects of the different circuit parameters may now be interpreted.

Impedance Level Variable, Q and Bias Fixed

Equations (80) and (81) show explicitly that the allowable vari-

ation in the external conductance and the width of the region defining near-sinusoidal oscillations are inversely proportional to K_z. This indicates that lowering the impedance level (decreasing K_z) increases the allowable range of operating points, and makes the operation of the circuit less critical.

An example of the improvement in waveshape which may be obtained by lowering the impedance level is shown by Figures 31 and 32. In both of these cases, the bias is held at 125 mv, (so that $G_d = G_{d\ max} = 6.6$ m℧) and the constant K_r selected so that $Q = 1/2Q_b$.

Even though the waveshape of Figure 31 qualifies via inequality (75) as being near-sinusoidal, the troughs of the wave are skewed, and the limit cycle is distorted due to the rapid changes in slope during the negative-going half cycle. The waveshape and limit cycle of Figure 32 show the effect of lowering the impedance level: The skewing in the troughs is considerably reduced, and the changes in the slope of the waveform are less abrupt as shown by the smoother limit cycle.

The effect of lowering K_z can also be shown with the aid of simple load line constructions on the diode characteristic. In terms of the base values of the circuit parameters, the equivalent shunt conductance of the tank circuit is

$$G = \frac{K_r}{K_z^2}\frac{R_b C_b}{L_b} = \frac{K_r}{K_z^2}(G_b) \ . \qquad (82)$$

Equation (82) may be rewritten as

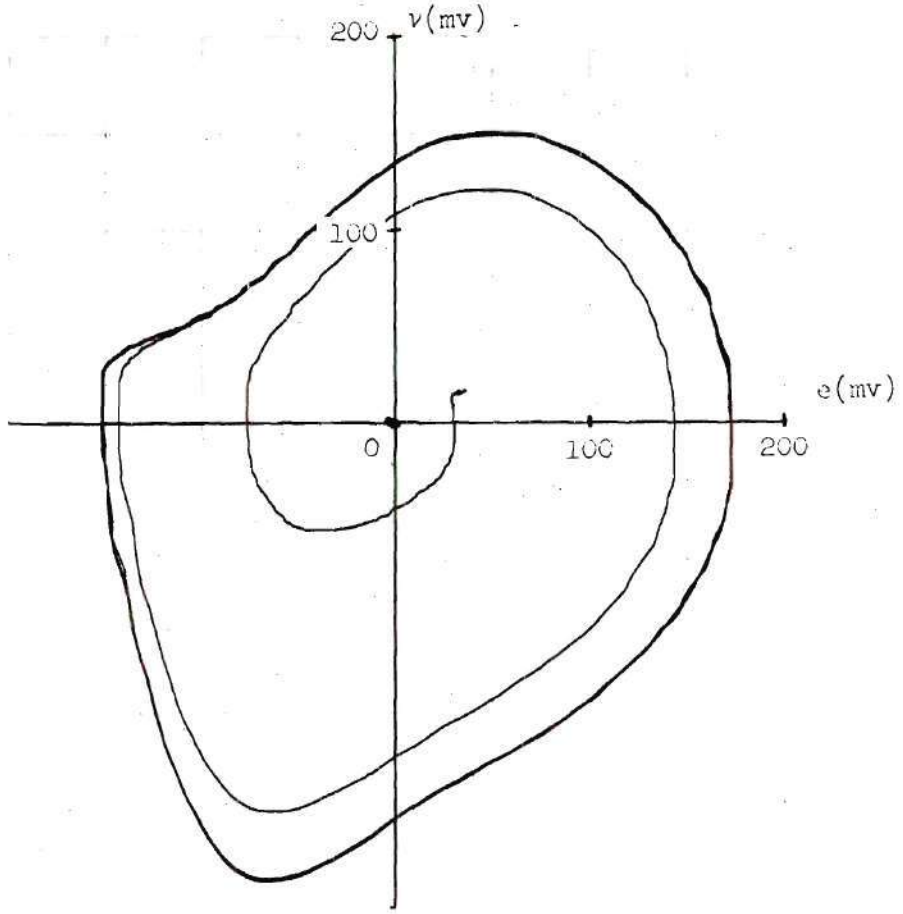

Figure 31(a). Phase Trajectory for $K_z = 1$, $K_r = 2$, ($Q = 1/2\ Q_b$) and Bias = 125 mv.

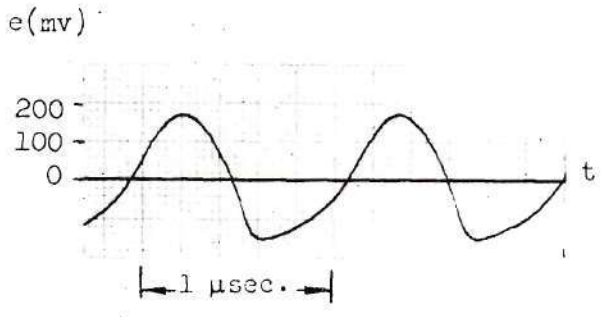

Figure 31(b). Instantaneous Waveform for $K_z = 1$, $K_r = 2$, ($Q = 1/2\ Q_b$) and Bias = 125 mv.

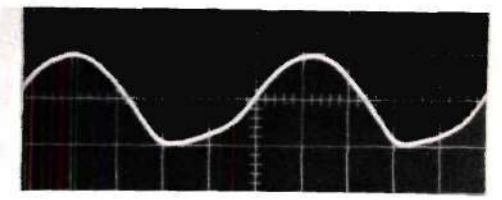

V: 150 mv/cm. H: 0.2 μsec/cm.

Figure 31(c). Output of Prototype Oscillator for $K_z = 1$, $K_r = 2$, ($Q = 1/2\ Q_b$) and Bias = 125 mv.

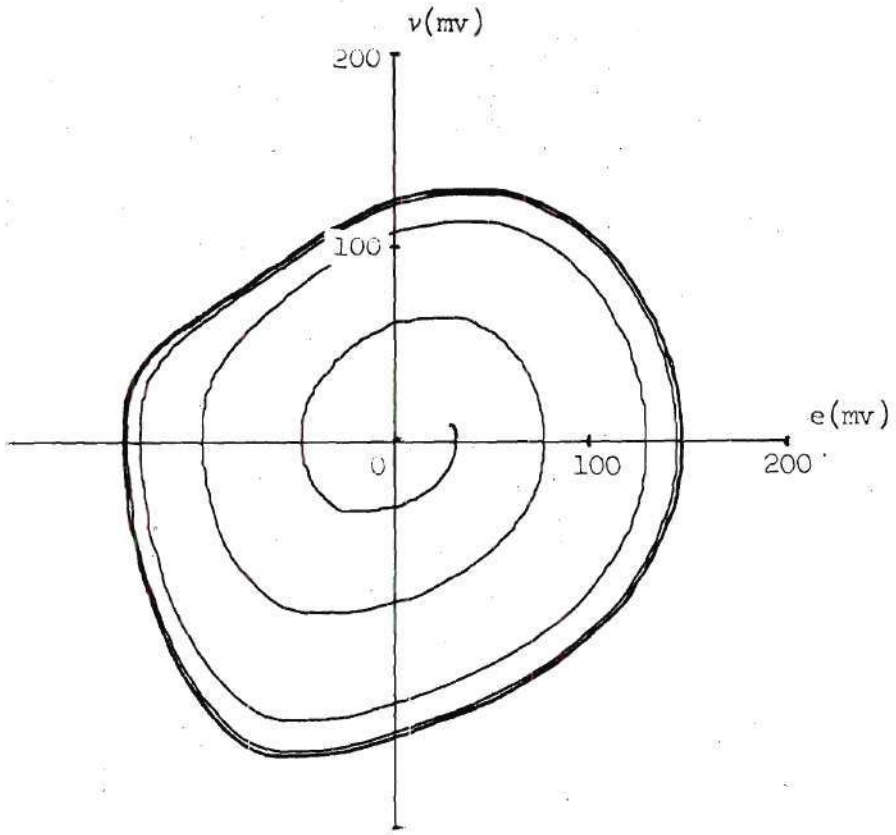

Figure 32(a). Phase Trajectory for $K_z = 1/2$, $K_r = 1$, ($Q = 1/2\ Q_b$) and Bias = 125 mv.

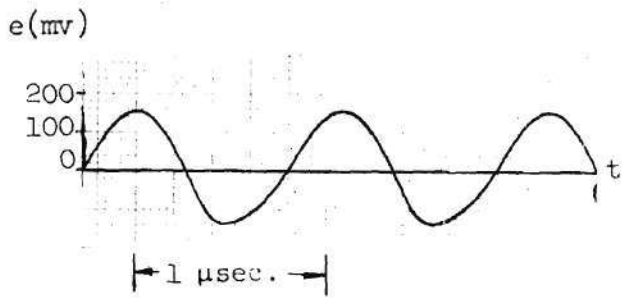

Figure 32(b). Instantaneous Waveform for $K_z = 1/2$, $K_r = 1$, ($Q = 1/2\ Q_b$) and Bias = 125 mv.

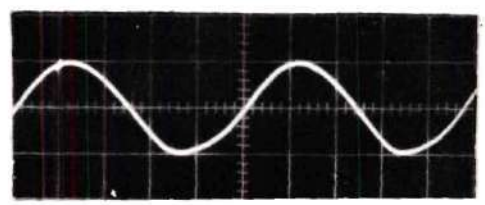

V: 150 mv/cm. H: 0.2 μsec/cm.

Figure 32(c). Output of Prototype Oscillator for $K_z = 1/2$, $K_r = 1$, ($Q = 1/2\ Q_b$) and Bias = 125 mv.

$$G = \frac{1}{K_z}\sqrt{\frac{C_b}{L_b}}\left(\frac{K_r}{K_z}R_b\sqrt{\frac{C_b}{L_b}}\right) \tag{83}$$

$$= \frac{1}{K_z}\sqrt{\frac{C_b}{L_b}}\left(\frac{1}{Q}\right).$$

The dynamic load line, of slope -G, is shown superimposed on the diode characteristic in Figure 33.

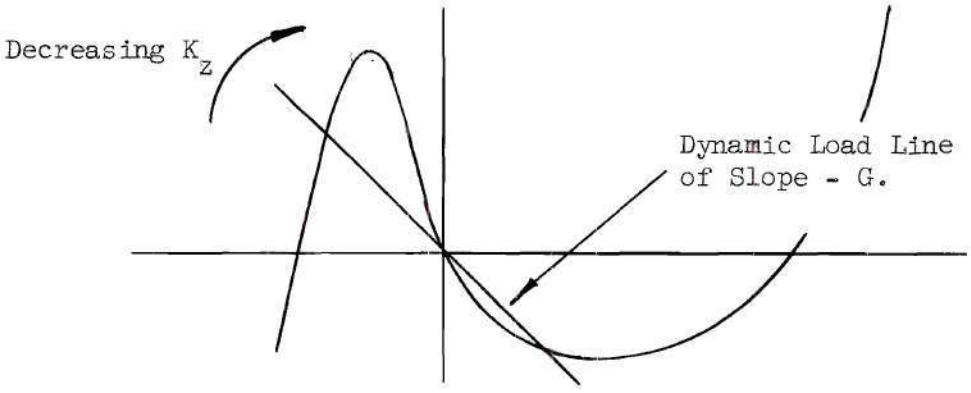

Figure 33. Effect of K_z on Dynamic Load Line for Fixed Bias and Constant Q.

For near-sinusoidal operation, as discussed earlier, the dynamic load line should be very nearly tangent to the diode characteristic at the bias point. From equation (82), it is apparent that a decrease in K_z will cause an increase in the magnitude of G and thus bring the load line nearer to tangency with the diode characteristic. Changing K_z alone, however, will also cause the circuit Q to change, in accordance with the original definition of Q. Equation (83) shows that, because K_z appears to the second power in the expression for G, it is possible to vary K_r in such a manner as to hold the circuit Q constant in the face of changes

in the impedance level. It is therefore possible to hold the bias and circuit Q constant and still effect an improvement in the waveshape by lowering the impedance level.

Q Variable, Bias and Impedance Level Fixed

The effect of changing the circuit Q while holding the bias and impedance level fixed can be seen with the aid of inequality (75). An increase of K_r will cause the left side of inequality (75) to approach an equality. Thus it is possible to increase K_r until

$$\frac{K_r}{K_z^2} (G_b) \equiv G_d \quad . \tag{84}$$

If the condition indicated by equation (84) is fulfilled, the equivalent shunt conductance of the tank circuit takes on its maximum allowable value, corresponding to point A in Figure 30, and ideally the waveshape is a perfect sinusoid. Since an increase in K_r corresponds to a decrease in the circuit Q, it is obvious that for fixed bias and impedance level, the waveshape is improved by lowering the circuit Q.

An example of the improvement in the waveshape which may be obtained by lowering the circuit Q is shown by Figures 34 and 35. In both of these cases, the bias is fixed at 125 mv, and K_z is unity. In Figure 34, the waveshape is skewed in the troughs, and the limit cycle possesses the corresponding distortions. In Figure 35, the Q has been reduced by a factor of 50. The waveshape is much closer to being sinusoidal, and the limit cycle is approaching an ellipse.

The effect of the circuit Q on the operation of the circuit can also be seen with the aid of a load line construction. Equation (83)

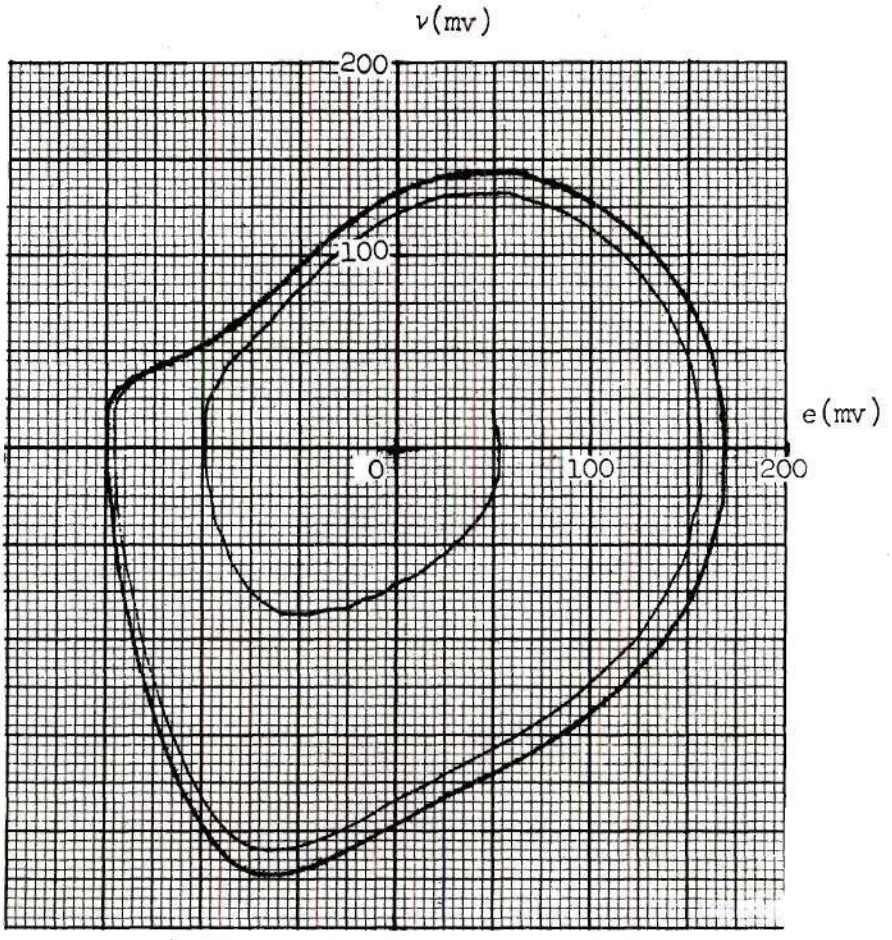

Figure 34(a). Phase Trajectory for $K_z = 1$, $K_r = 1$, $(Q = Q_b)$ and Bias = 125 mv.

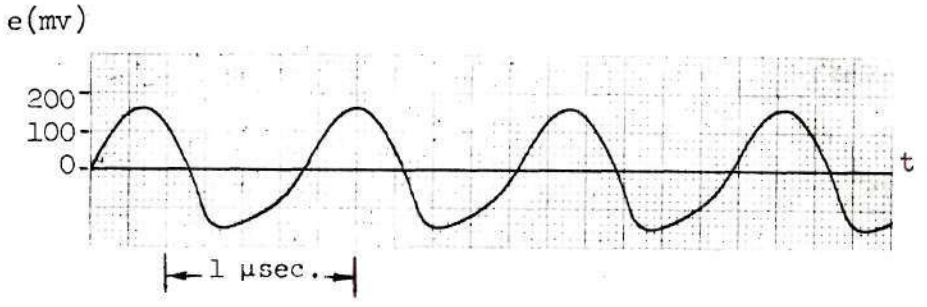

Figure 34(b). Instantaneous Waveform for $K_z = 1$, $K_r = 1$, $(Q = Q_b)$ and Bias = 125 mv.

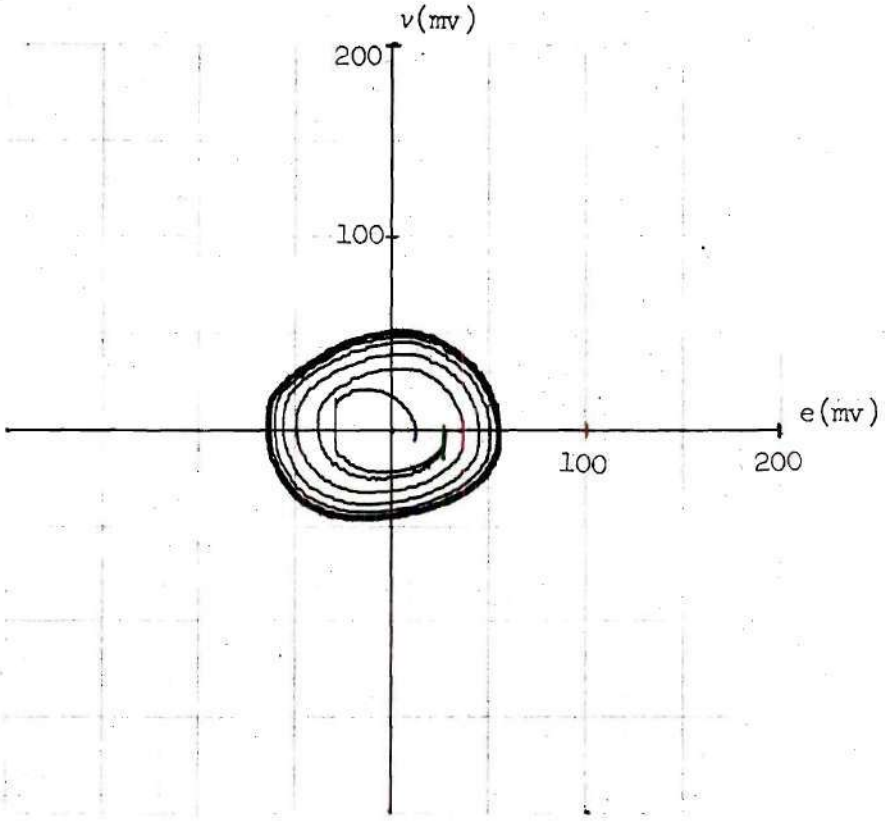

Figure 35(a). Phase Trajectory for $K_z = 1$, $K_r = 50$, ($Q = 1/50\ Q_b$), and Bias = 125 mv.

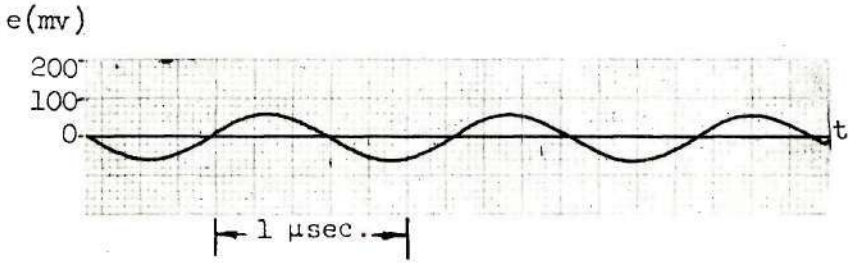

Figure 35(b). Instantaneous Waveform for $K_z = 1$, $K_r = 50$, ($Q = 1/50\ Q_b$), and Bias = 125 mv.

shows that the slope of the dynamic load line is inversely proportional to the circuit Q. Therefore, if the Q is lowered by an increase in K_r, the magnitude of the slope will increase and, as shown in Figure 36, the dynamic load line will rotate closer to tangency with the diode characteristic.

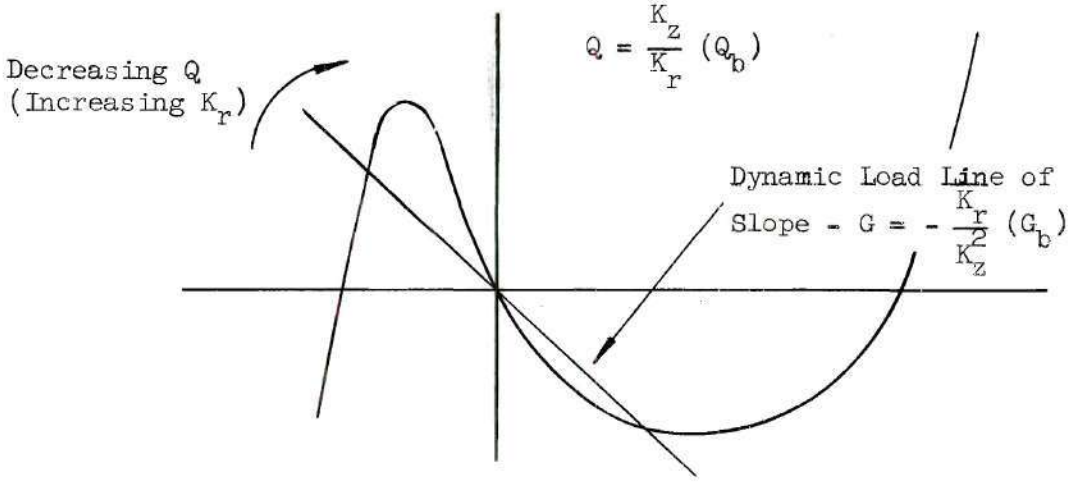

Figure 36. Effect of Circuit Q on Dynamic Load Line for Fixed Bias and Impedance Level.

In the light of inequality (75), equation (83) and Figures 34, 35, and 36, it is therefore possible to hold the bias and impedance level fixed and effect an improvement in the waveshape by lowering the circuit Q.

Bias Variable, Impedance Level and Q Fixed

In the preceding analysis, it has been assumed that the incremental conductance of the diode is essentially constant throughout the dynamic range of the operating point. The range for which this is true is very limited, even for small amplitudes of oscillation, as shown in Figure 37. The preceding analysis is most accurate when the bias is chosen near the

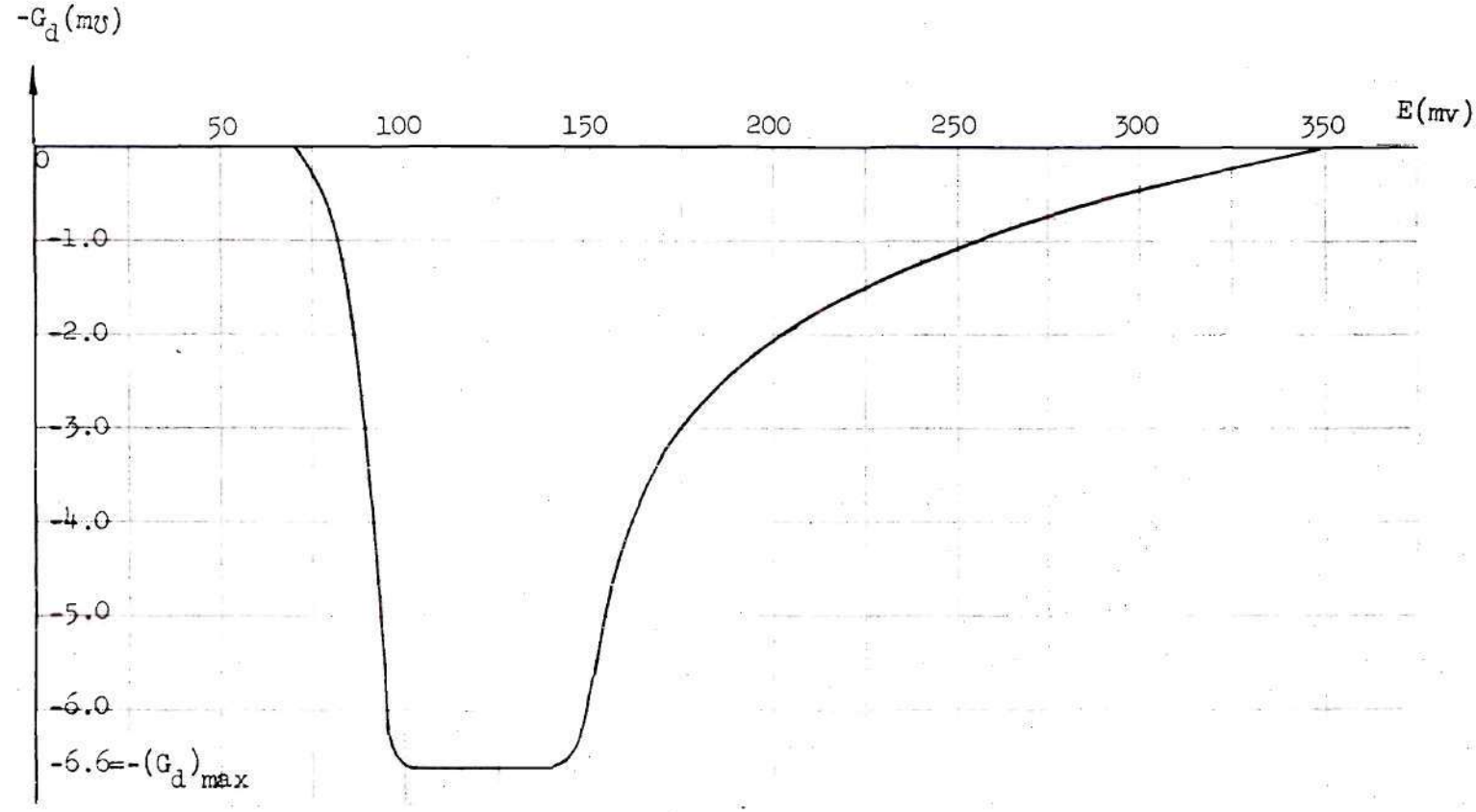

Figure 37. Variation of Diode Incremental Conductance.

center of the linear region to allow for approximately equal voltage swings of the instantaneous operating point.

The most obvious effect the bias point can have on the circuit operation is whether or not it meets the conditions for self-starting and sustained oscillations. As previously discussed, for the circuit to be self-starting, it must be true that

$$G_d > \frac{K_r}{K_z^2} (G_b) . \tag{85}$$

It is obvious, then, that for a fixed value of K_z and K_r there is a fixed range of bias points which allow self-starting and sustained oscillations. The allowable range of bias points for different combinations of K_z and K_r is shown in Figure 38.

The information contained in Figure 38 may also be interpreted in the light of the load line constructions given earlier. For a fixed value of K_z and K_r, the magnitude of the slope of the dynamic load line is fixed. As shown in Figure 39, changing the bias point will then shift the load line on the diode characteristic. At points 1 and 2, G_d is greater than G, and the oscillator is self-starting. At point 3, G_d is less than G, and the oscillator is not self-starting. The points 4 and 5 correspond to the threshold condition where the slope of the dynamic load line is just equal to that of the diode characteristic. The points shown in Figure 39 are also labeled in Figure 38 as an example for the case corresponding to a load line where $K_z = 1/4$ and $K_r = 2$.

Inspection of Figures 38 and 39 shows that, as the slope of the dynamic load line is increased so that it approaches the maximum slope

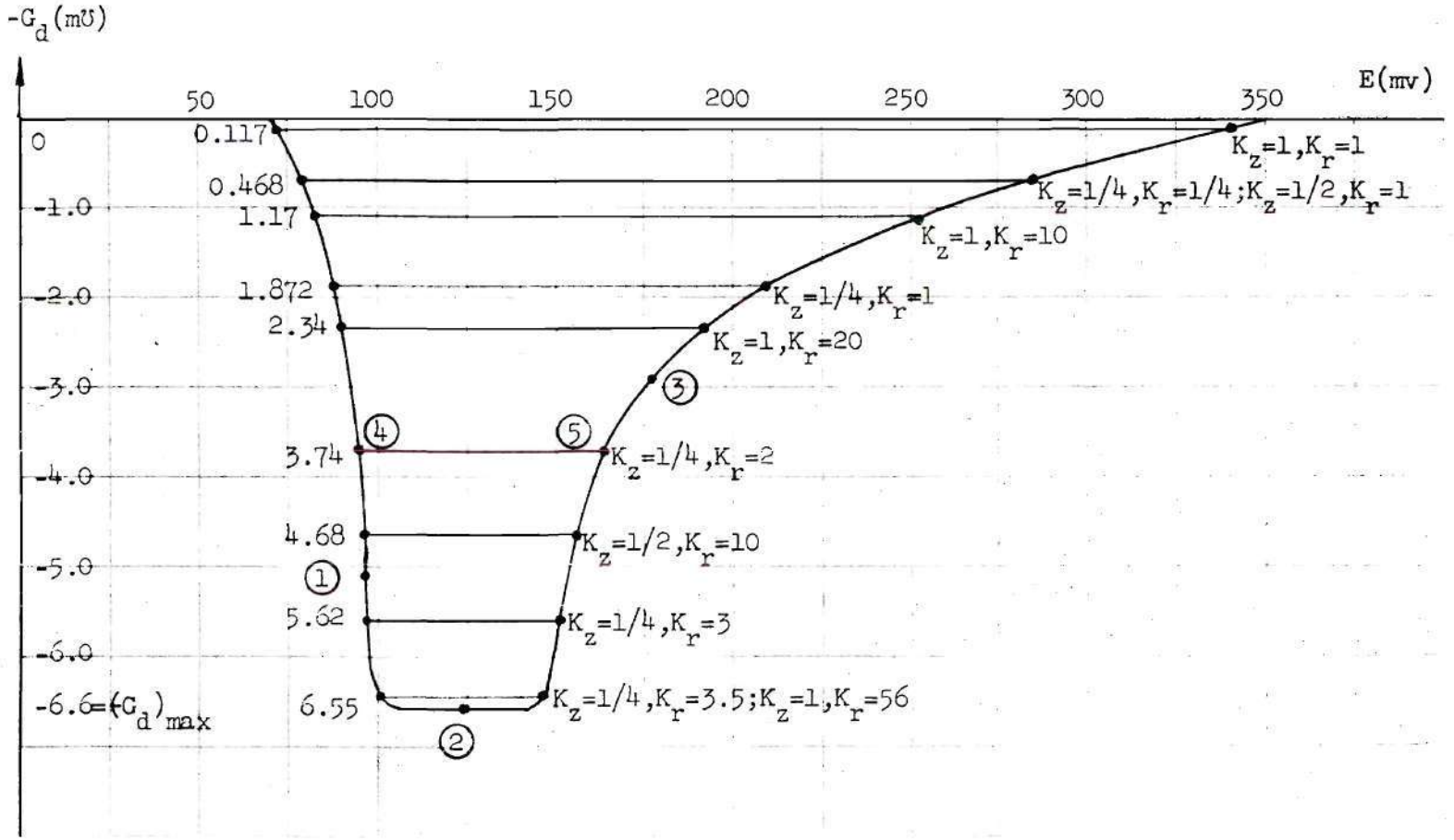

Figure 38. Allowable Range of Bias Points for Various Combinations of K_z and K_r.

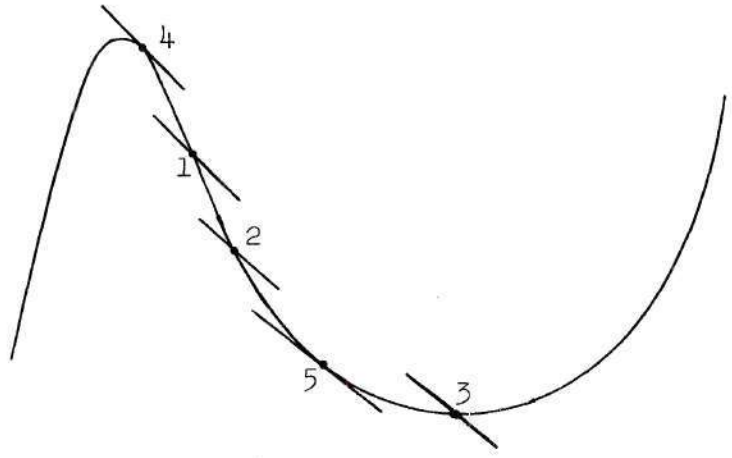

Figure 39. Various Bias Points for a Given Dynamic Load Line.

of the diode characteristic, the threshold points 4 and 5 move closer together with point 5 moving the greater distance due to the asymmetry of the characteristic. The possible range of bias values for self-starting conditions thus decreases with an increase in the slope of the dynamic load line.

Another aspect of the effect of the bias on the circuit operation is its role in the distortion of the waveshape.

One form of distortion, as shown in earlier sections, is a skewing effect in the troughs of the waveform. This skewing of the troughs may be explained heuristically by the following: The equivalent circuit of the oscillator, shown in Figure 40, may be thought of as containing a shunt conductance which is the composite of the diode conductance and the equivalent shunt conductance of the tank circuit. The volt-ampere characteristic of this composite conductance is shown in Figure 41.

As discussed earlier, when oscillations build up in the circuit, the instantaneous operating point will eventually pass into a dissipative

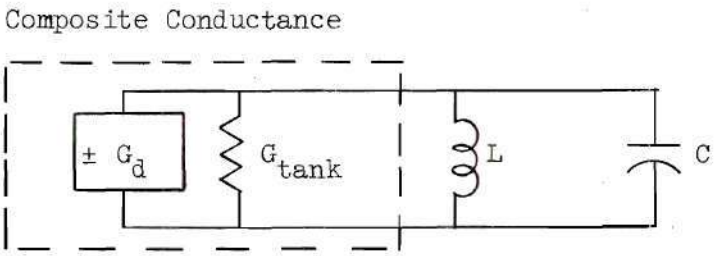

Figure 40. Equivalent Oscillator Circuit.

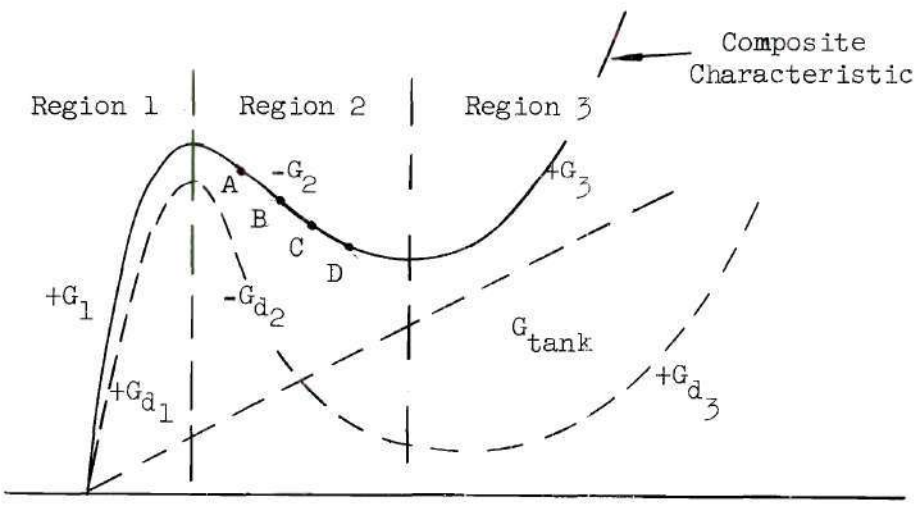

Figure 41. Composite Volt-Ampere Characteristic.

region of the characteristic during some portion of the cycle. The amplitude will limit when the energy lost is just equal to that supplied during a complete cycle. If the diode is biased, for example, at point A on the composite characteristic of Figure 41, the operating point will eventually swing into Region 1, and limiting will occur.

At this point, it is useful to consider the composite characteristic piecewise-linear, as shown in Figure 42, and investigate the behavior of the circuit in each region. The equation describing the circuit in any region is

$$\frac{d^2e}{dt^2} + \frac{G}{C}\frac{de}{dt} + \frac{1}{LC}\, e = 0 , \tag{86}$$

where

$$G = \pm G_{diode} + G_{tank}$$

$$= \pm G_d + \frac{K_r}{K_z^2}(G_b) \tag{87}$$

is the composite conductance of the region in question.

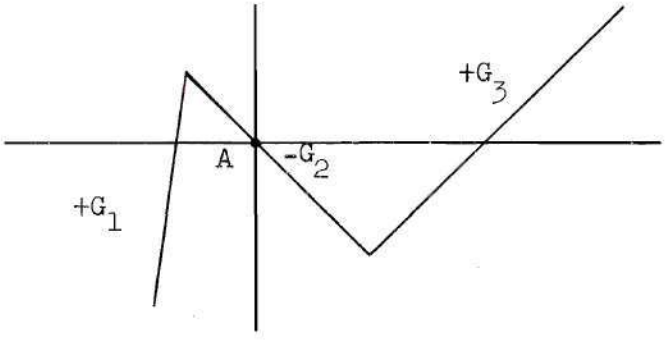

Figure 42. Piecewise-Linear Composite Characteristic.

Equation (86) is of the general form

$$\frac{d^2e}{dt^2} + 2\alpha\frac{de}{dt} + \omega_o^2\, e = 0 , \tag{88}$$

where

$$\alpha = \frac{G}{2C} , \tag{89}$$

and

$$\omega_o^2 = \frac{1}{LC} . \tag{90}$$

Substitution of equation (87) in equation (89) yields

$$\alpha = K_z \frac{(\pm G_d)}{2C_b} + \frac{K_r}{K_z}\left(\frac{G_b}{2C_b}\right). \tag{91}$$

The damping constant α may be written for each of the three regions of the composite characteristic as

$$\alpha_1 = K_z \frac{(+G_{d1})}{2C_b} + \frac{K_r}{K_z}\left(\frac{G_b}{2C_b}\right), \tag{92}$$

$$\alpha_2 = K_z \frac{(-G_{d2})}{2C_b} + \frac{K_r}{K_z}\left(\frac{G_b}{2C_b}\right), \tag{93}$$

and

$$\alpha_3 = K_z \frac{(+G_{d3})}{2C_b} + \frac{K_r}{K_z}\left(\frac{G_b}{2C_b}\right). \tag{94}$$

When the instantaneous operating point is driven into Region 1, the circuit then behaves as a lossy parallel GLC circuit in a mode governed by the relative magnitudes of α_1 and ω_o. From the diode characteristic, $+G_{d1}$ may be approximated as +20 m℧. Substitution of numerical values in equation (92) yields

$$\alpha_1 = K_z(+5.7 \times 10^6) + \frac{K_r}{K_z}(0.033 \times 10^6). \tag{95}$$

For $K_z = K_r = 1$,

α_1 becomes

$$\alpha_1 = +5.733 \times 10^6 . \tag{96}$$

The constant ω_o is

$$\omega_o = \frac{1}{\sqrt{LC}} = \frac{1}{\sqrt{L_b C_b}} = 6.16 \times 10^6 . \qquad (97)$$

Since $\alpha_1 < \omega_o$ the circuit operates in Region 1 in the underdamped mode with positive damping, and the output is of the form

$$e_1(t) = A\epsilon^{-\alpha_1 t} \sin(\beta_1 t + \theta) , \qquad (98)$$

where

$$\beta_1 = \sqrt{\omega_o^2 - \alpha_1^2} . \qquad (99)$$

Equations (98) and (99) may now be used to explain the skewing effect previously encountered. Since the damped frequency β_1 is less than the frequency ω_o, the waveform will "spread" in frequency when the operating point moves into Region 1. This situation is illustrated in Figure 43.

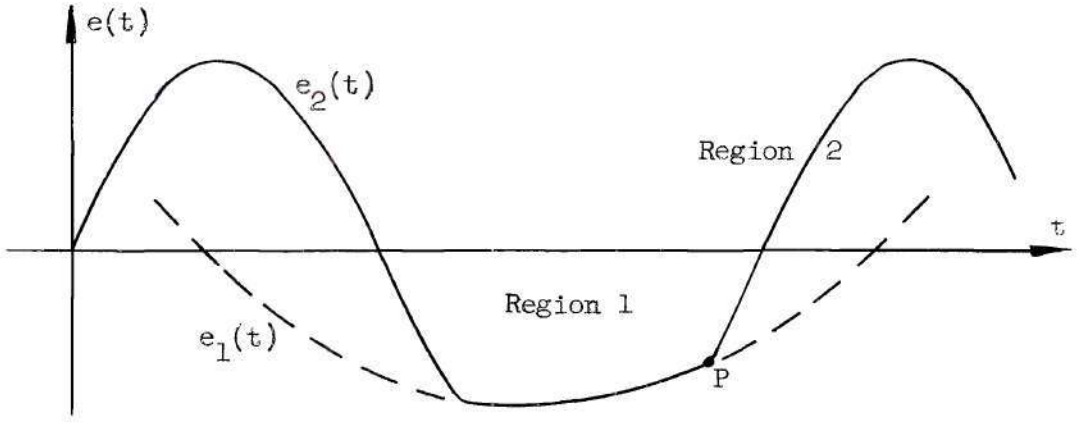

Figure 43. Skew Distortion of Output Waveshape.

The point P in Figure 43 represents the point at which the operating

point moves back into Region 2 and the circuit changes its mode of operation to that of a negative resistance oscillator.

Before proceeding with the discussion of the influence of the bias point on the waveshape, it is interesting to re-examine some of the earlier conclusions on the effects of impedance level and circuit Q on the distortion of the waveshape. Figures 31 and 32 illustrate the effect of lowering the impedance level with Q held constant. For Figure 31, the damping constant in Region 1 is

$$(\alpha_1)_{31} = 5.766 \times 10^6 , \tag{100}$$

while in Figure 32 the damping constant for Region 1 is

$$(\alpha_1)_{32} = 2.916 \times 10^6 . \tag{101}$$

From equation (99), it is obvious that

$$(\beta_1)_{32} = \sqrt{\omega_o^2 - (\alpha_1)_{32}^2} > (\beta_1)_{31} = \sqrt{\omega_o^2 - (\alpha_1)_{31}^2} . \tag{102}$$

In other words, lowering the impedance level has made $(\beta_1)_{32}$ closer to the natural frequency, ω_o, than is $(\beta_1)_{31}$. Hence, for the lower impedance level, the "spread" in frequency is reduced, and the operating point may be thought of as spending less time in Region 1 thereby reducing the skewing effect. Figures 34 and 35 illustrate the effects of lowering the circuit Q while holding the impedance level constant. For Figure 34 the damping constant in Region 1 is

$$(\alpha_1)_{34} = 5.733 \times 10^6 , \tag{103}$$

while in Figure 35, the damping constant is

$$(\alpha_1)_{35} = 7.35 \times 10^6 . \qquad (104)$$

In this case, lowering Q (increasing K_r) causes the "spread" in frequency to increase since

$$(\beta_1)_{35} = \sqrt{\omega_o^2 - (\alpha_1)_{35}^2} < (\beta_1)_{34} = \sqrt{\omega_o^2 - (\alpha_1)_{34}^2} . \qquad (105)$$

It must be remembered, however, that the waveshape in Region 1 is a damped sinusoid, and the damping constant $(\alpha_1)_{35}$ is greater than $(\alpha_1)_{34}$. That is, lowering the circuit Q causes the damped frequency to decrease but the damping constant is increased. This has the effect of causing the voltage to decay toward Region 2 at a more rapid rate. Thus, the operating point spends less time in Region 1, and the skewing effect is reduced.

The effect of the bias point on the distortion of the waveshape can be approached by a consideration of the energy balance in the circuit. Thus far, it has been assumed that the waveform is limited only by Region 1 of the composite characteristic. If the bias point is moved toward the valley of the characteristic, the instantaneous operating point may enter both Region 1 and Region 3 before steady state limiting occurs. How far into these dissipative regions it goes depends of course on the amount of energy stored in the reactive elements during the cycle. The amplitude limits when the energy dissipated is just equal to that stored over a complete cycle.

Since the composite characteristic of Figure 41 is asymmetrical as well as nonlinear, the degree of limiting in Regions 1 and 3 will be different. For small excursions outside of Region 2, the waveshape will experience rather abrupt limiting in Region 1, since the incremental con-

ductance changes sharply from $-G_2$ to $+G_1$. The degree of limiting offered by Region 3 depends more on the amplitude of the waveform than in Region 1. Passing from Region 2 to Region 3, the incremental conductance changes slowly from $-G_2$ to $+G_3$. For small excursions into Region 3, the incremental conductance is small and approaches that of Region 1 only if the excursion into Region 3 is sufficiently large.

When the instantaneous operating point is driven into Region 3, the waveshape experiences a distortion of its peaks much like that associated with its troughs and Region 1. Since the limiting in Region 3 is relatively gentle compared to that of Region 1, the distortion of the peaks is much less objectionable for equal excursions into both regions. Because the composite characteristic is asymmetrical, the amplitude of oscillation does not reach a maximum when the bias point is selected in the most linear region. The reason for this is the fact that the limiting is asymmetrical. If the bias is fixed at point A of Figure 41, the amplitude will build up until the operating point encounters Region 1 and limiting occurs. If the bias point is moved to point B, the amplitude must reach a higher level before sufficient limiting occurs to invoke the steady state, and Region 3 begins to take a small part in the overall limiting action. If, however, the bias point is moved further into the valley of the composite characteristic, say to point C of Figure 41, the amplitude will increase even further. This is due to the fact that as the oscillations build up, the initial amount of dissipation in Region 3 is too small to effect limiting, and the amplitude must increase even further. It will eventually reach a level such that the instantaneous operating point will swing further into Region 3 and also into Region 1

in order to accomplish the net dissipation required to invoke steady state operation. The required excursion into Region 1 is now smaller than before, and the distortion of the troughs of the waveshape is reduced. Since the excursion into Region 3 is increased, the distortion of the peaks of the waveshape now becomes apparent. If the bias point is moved further toward the valley of the characteristic, say to point D, the steady state amplitude will begin to decrease. As the valley is approached, the incremental conductance is getting smaller and the energy supplied to the circuit for small amplitudes is decreasing. Hence, the gentle limiting of Region 3 is adequate to establish the steady state with no involvement of Region 1. At this stage, the distortion of the waveshape is almost entirely in the peaks.

An example showing this sequence of bias points and the associated waveshapes is given by Figures 44 through 47.

Overall Effect of the Circuit Parameters

The overall effect of the circuit parameters on the waveshape for the case of near-sinusoidal oscillations can be summarized with the aid of equation (29) of Chapter II. Thus far, it has been noted that the waveshape is improved by:

(a) Lowering the impedance level (decreasing K_z), when the circuit Q (K_z/K_r ratio) and bias point (value of G_d) are fixed.

(b) Lowering the circuit Q (increasing K_r) when the impedance level (K_z) and bias (G_d) are fixed.

(c) Increasing the bias (decreasing the magnitude of G_d) when the impedance level and circuit Q are fixed.

From equation (29) of Chapter II, the real part of the system roots is expressed as

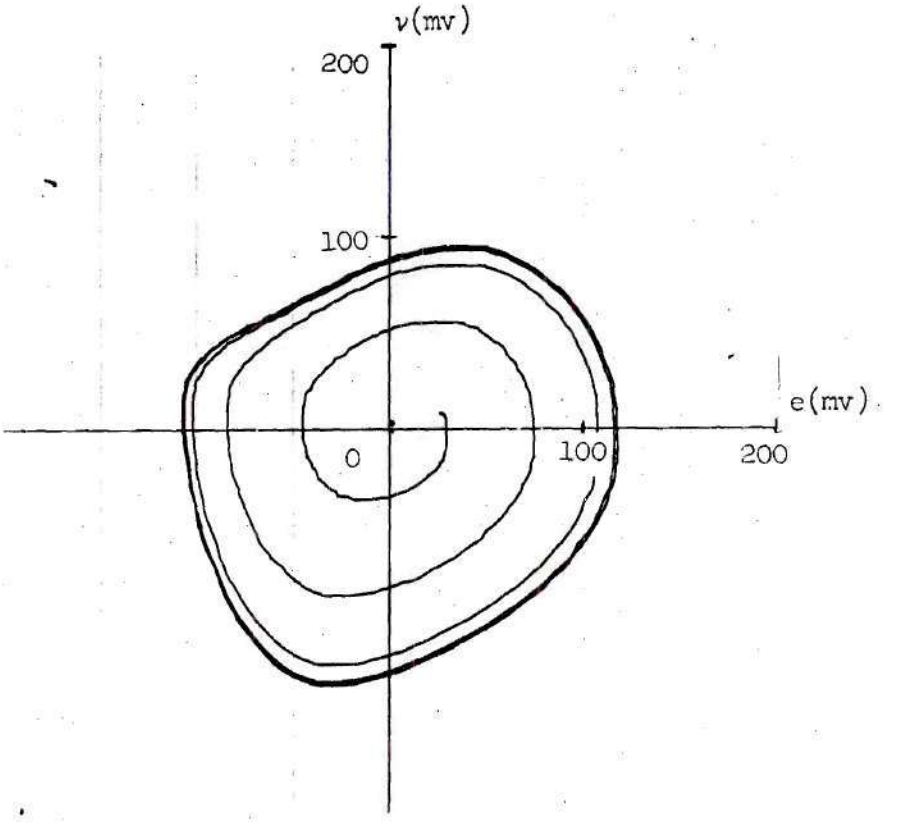

Figure 44(a). Phase Trajectory for $K_z = 1/2$, $K_r = 10$, and Bias Point A = 100 mv.

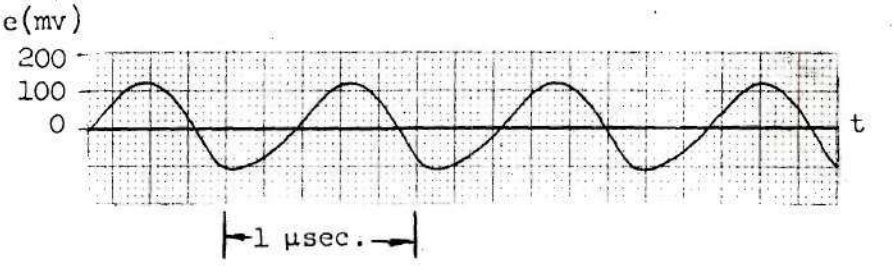

Figure 44(b). Instantaneous Waveform for $K_z = 1/2$, $K_r = 10$, and Bias Point A = 100 mv.

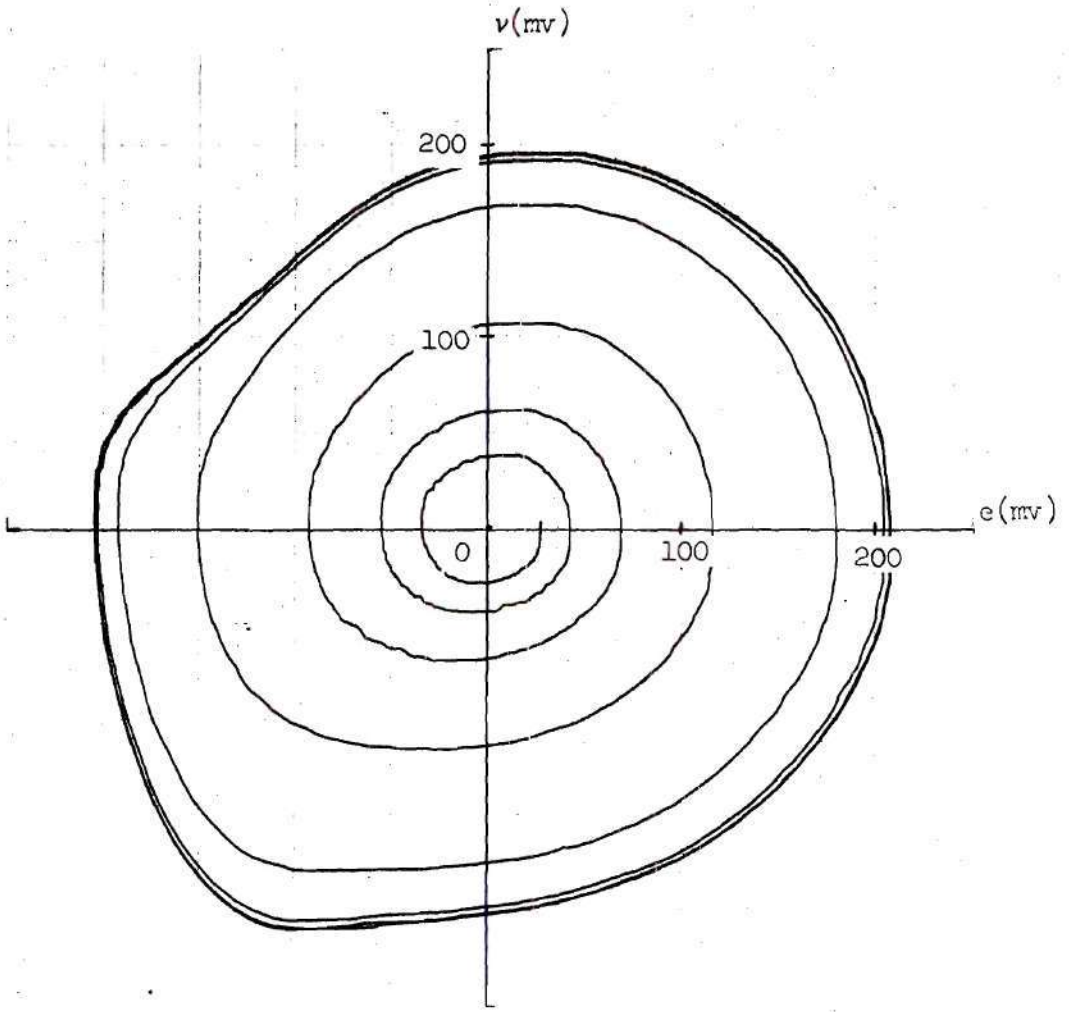

Figure 45(a). Phase Trajectory for $K_z = 1/2$, $K_r = 10$, and Bias Point B = 180 mv.

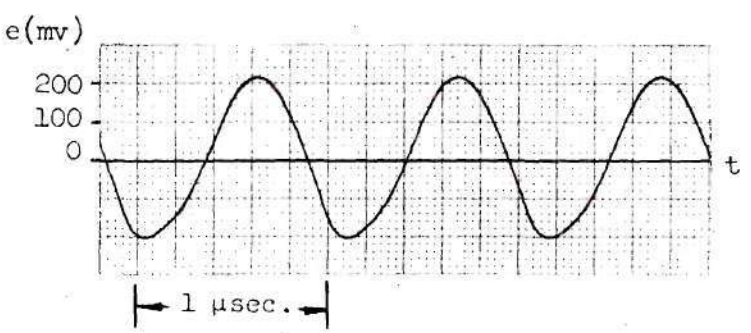

Figure 45(b). Instantaneous Waveform for $K_z = 1/2$, $K_r = 10$, and Bias Point B = 180 mv.

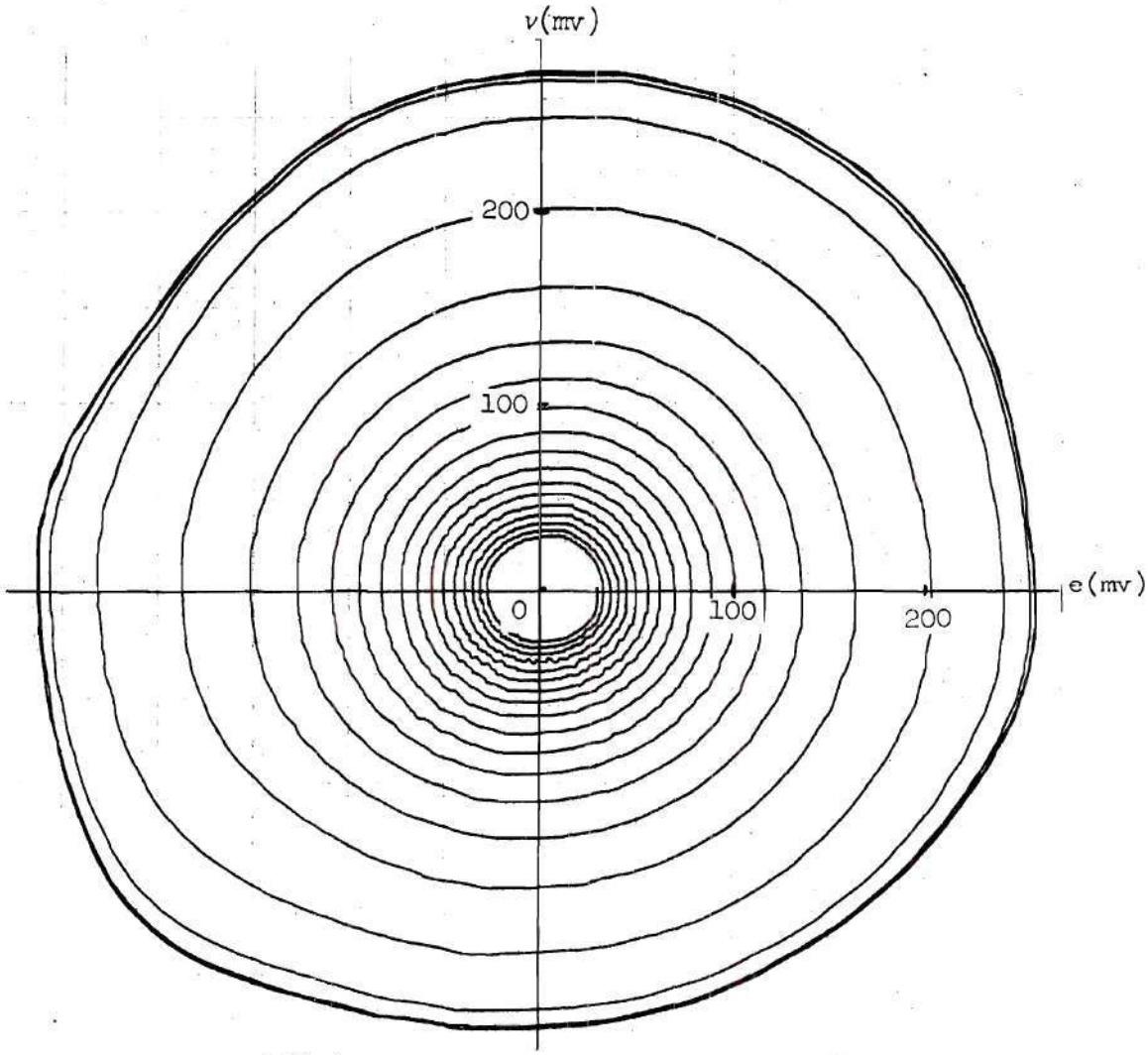

Figure 46(a). Phase Trajectory for $K_z = 1/2$, $K_r = 10$, and Bias Point C = 250 mv.

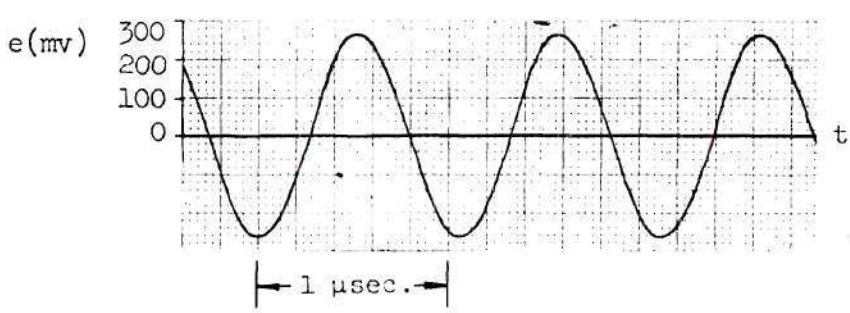

Figure 46(b). Instantaneous Waveform for $K_z = 1/2$, $K_r = 10$, and Bias Point C = 250 mv.

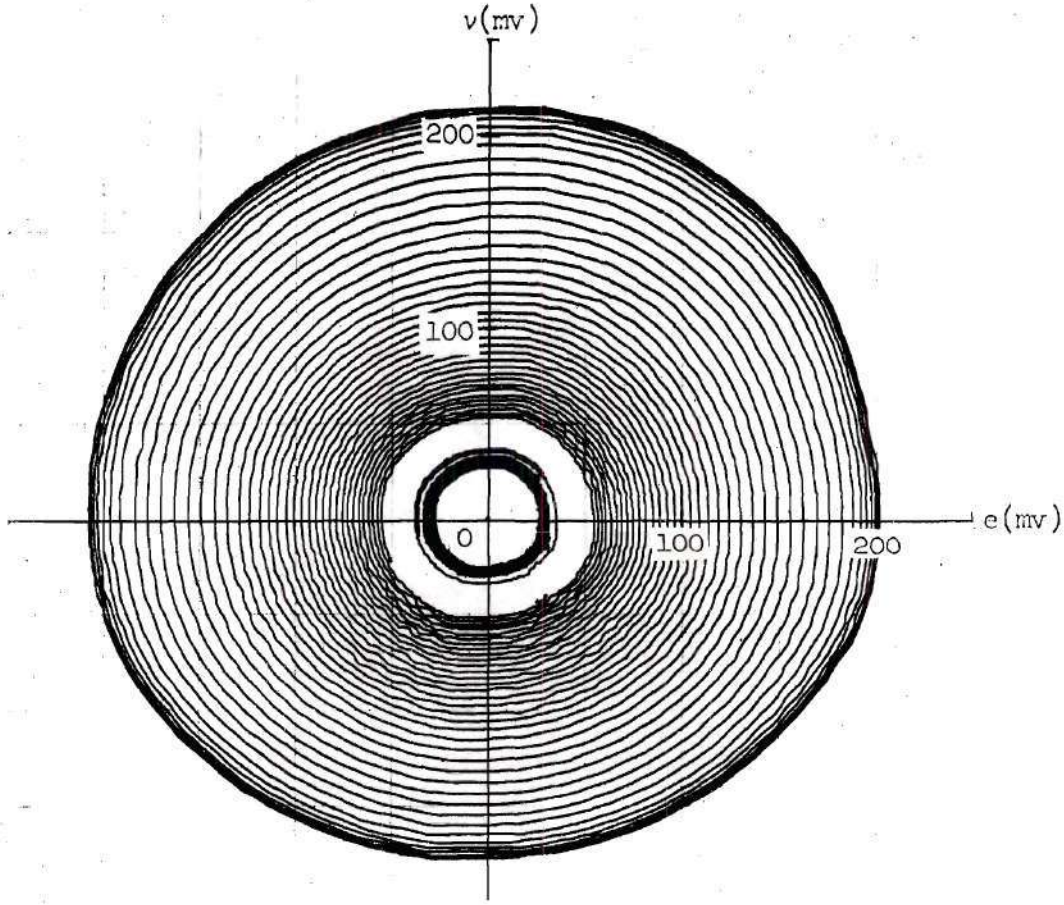

Figure 47(a). Phase Trajectory for $K_z = 1/2$, $K_r = 10$, and Bias Point D = 300 mv.

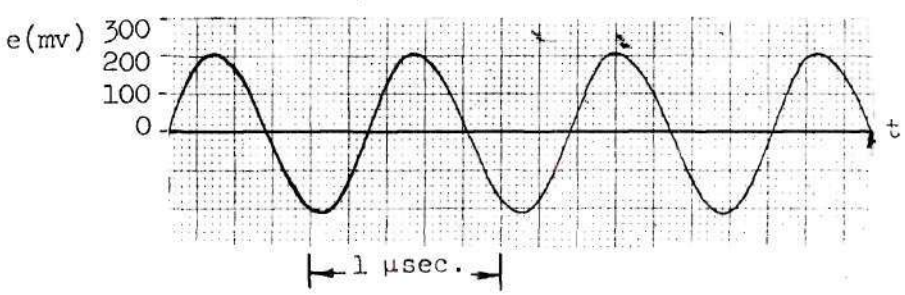

Figure 47(b). Instantaneous Waveform for $K_z = 1/2$, $K_r = 10$, and Bias Point D = 300 mv.

$$\alpha = -\frac{1}{2C} (G - G_d) . \tag{106}$$

The term in parentheses is expressible as

$$(G - G_d) = \frac{K_r}{K_z^2} (G_b) - G_d$$

$$= \frac{1}{K_z} \left(\frac{K_r}{K_z} \right) G_b - G_d . \tag{107}$$

For growing oscillations it must be true that

$$G_d > \frac{1}{K_z} \left(\frac{K_r}{K_z} \right) G_b , \tag{108}$$

and the limiting case of ideal sinusoidal oscillations is reached when

$$G_d = \frac{1}{K_z} \left(\frac{K_r}{K_z} \right) G_b . \tag{109}$$

Inspection of inequality (108) shows that an improvement of the waveshape by (a), (b), or (c) as stated above amounts to the same thing in terms of the system behavior: making the real part of the system roots approach zero. In other words, steps (a), (b), or (c) result in making inequality (108) approach the equality in equation (109) thereby moving the system roots nearer to the $j\omega$-axis and the system behavior closer to sinusoidal in the steady state.

If the desired sinusoidal waveshape is approached from the system root standpoint, the required relationship between the circuit parameters

may be found. By way of example, it is assumed that the bias is fixed in the most linear region (125 mv) so that the incremental conductance of the diode is $(G_d)_{max}$. The relation between K_r and K_z is then found from equation (109). For the base values of the circuit parameters and $(G_d)_{max} = 6.6$ m℧, equation (109) becomes

$$\frac{K_r}{K_z^2} = 56.5 , \tag{110}$$

and this represents the threshold condition of perfect sinusoidal oscillations.

Examples of the near-sinusoidal response are shown in Figures 48 and 49. Figure 48 represents the case where $K_z = 1$, and equation (110) says the threshold value of K_r is 56.5. The constant K_r was adjusted to 56 for Figure 48. Figure 49 represents a case where the circuit has been made less critical by lowering K_z to 1/4. Equation (110) says the threshold value of K_r is then 3.53. The constant K_r was adjusted to 3.5 for Figure 49. The improvement in the waveshape is evident from the fact that lowering the impedance level has made the limit cycle of Figure 49 almost a perfect circle.

Relaxation Oscillations

A detailed analysis of the circuit operation in a relaxation mode is beyond the scope of this work. It is interesting, however, to cite an example of relaxation oscillations and point out some of the eccentricities associated with this mode of circuit behavior.

In Chapter II, it was shown that if the circuit parameters take

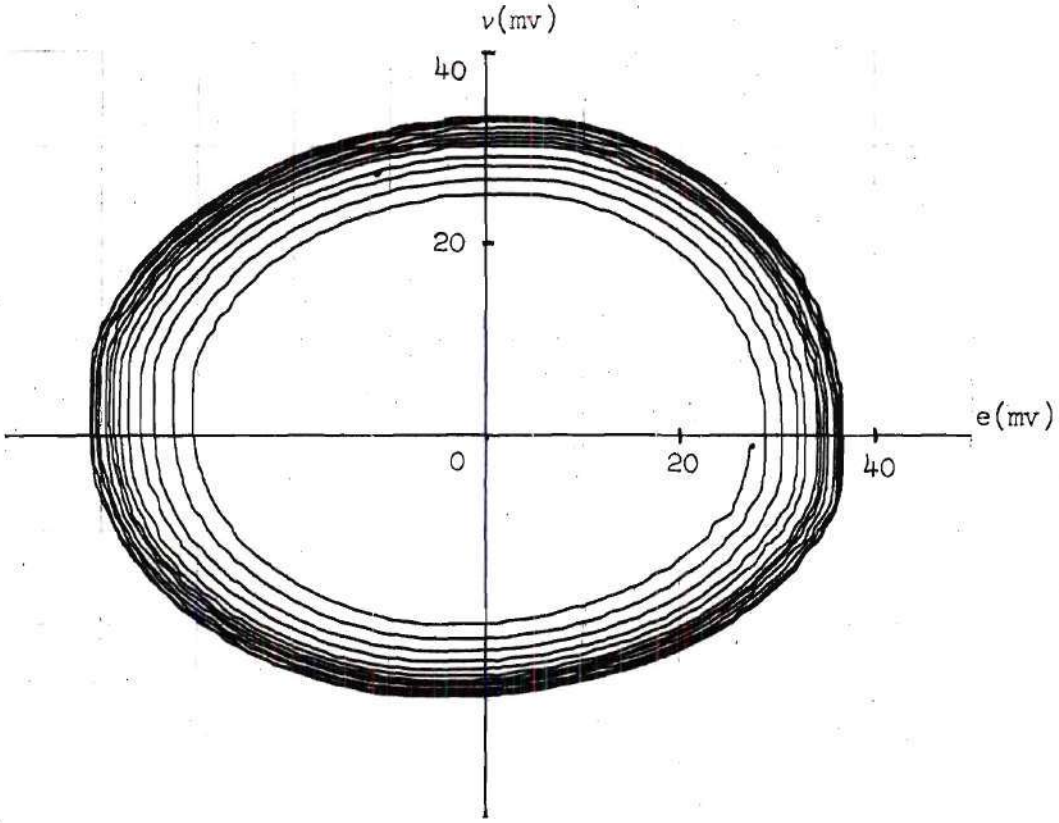

Figure 48(a). Phase Trajectory for $K_z = 1$, $K_r = 56$, and Bias = 125 mv.

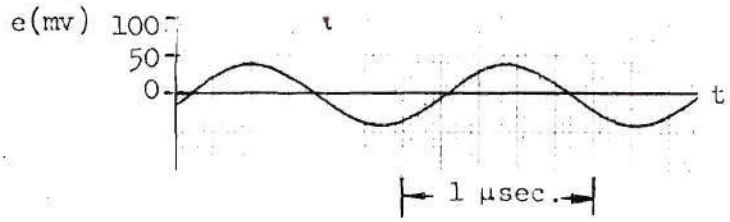

Figure 48(b). Instantaneous Waveform for $K_z = 1$, $K_r = 56$, and Bias = 125 mv.

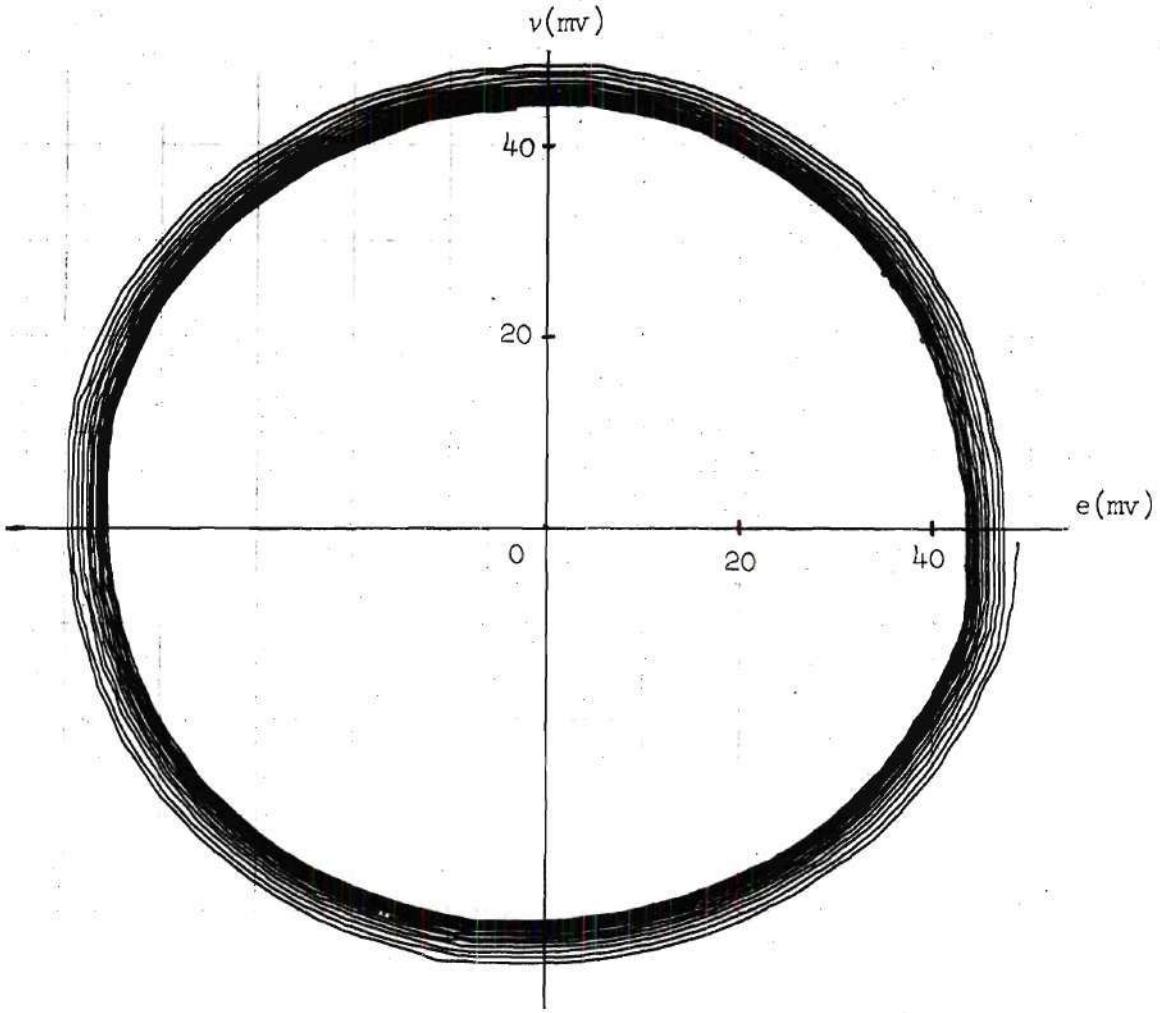

Figure 49(a). Phase Trajectory for $K_z = 1/4$, $K_r = 3.5$, and Bias = 125 mv.

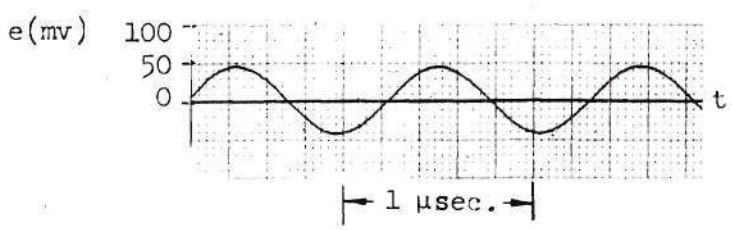

Figure 49(b). Instantaneous Waveform for $K_z = 1/4$, $K_r = 3.5$, and Bias = 125 mv.

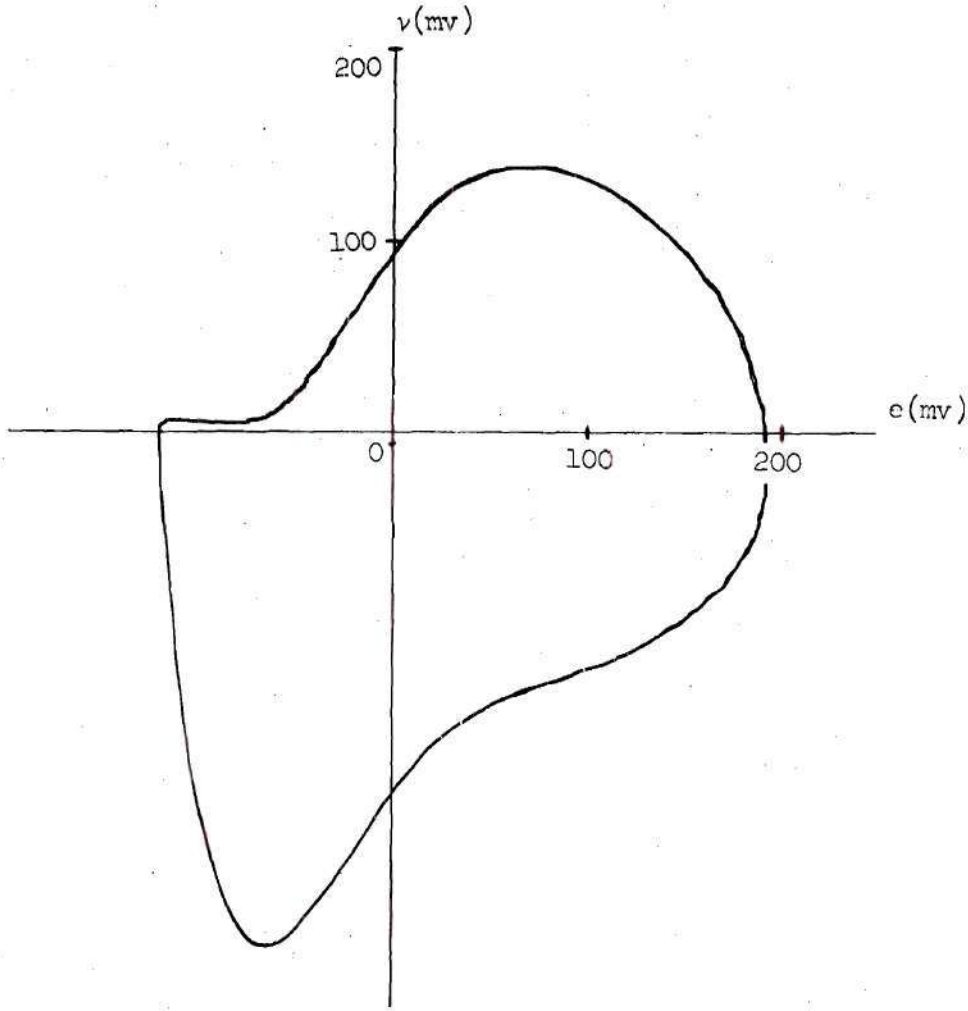

Figure 50(a). Phase Trajectory for $K_z = 3$, $K_r = 135$, and Bias = 125 mv.

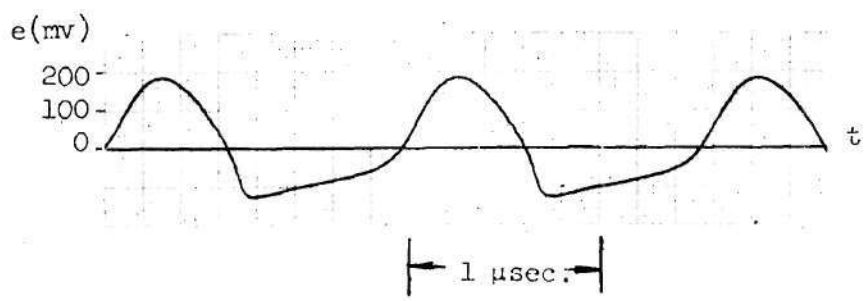

Figure 50(b). Instantaneous Waveform for $K_z = 3$, $K_r = 135$, and Bias = 125 mv.

on values such that

$$G_d > G \ , \tag{111}$$

and

$$\frac{4C}{L} < (G - G_d)^2 \ , \tag{112}$$

the circuit will operate as a relaxation oscillator.

An example of such a case is shown in Figure 50 where the bias is fixed at 125 mv so that $G_d = (G_d)_{max} = 6.6$ m℧, $K_z = 3$ and $K_r = 135$. The overall waveshape is grossly non-sinusoidal with the trough characterized by an almost linear ramp, and the limit cycle is highly distorted. The behavior in the trough of the waveshape can be explained with the aid of Figure 41 and equation (91) of the preceding section. In Region 1 of the composite characteristic the damping constant is

$$\alpha_1 = 18.585 \times 10^6 \ . \tag{113}$$

In this case $\alpha_1 > \omega_o$, and the circuit operates as a lossy parallel GLC circuit in the overdamped mode as long as the instantaneous operating point remains in Region 1. Hence, the output, after going negative, will approach zero approximately as an exponential curve until the instantaneous operating point moves back into Region 2 where the damping constant changes sign. This effect is illustrated in Figure 51.

In addition to this markedly nonsinusoidal behavior, it was noticed that in some cases the oscillator was not self-starting when the bias point was near the valley of the characteristic unless the initial conditions were above some critical value. This is an interesting

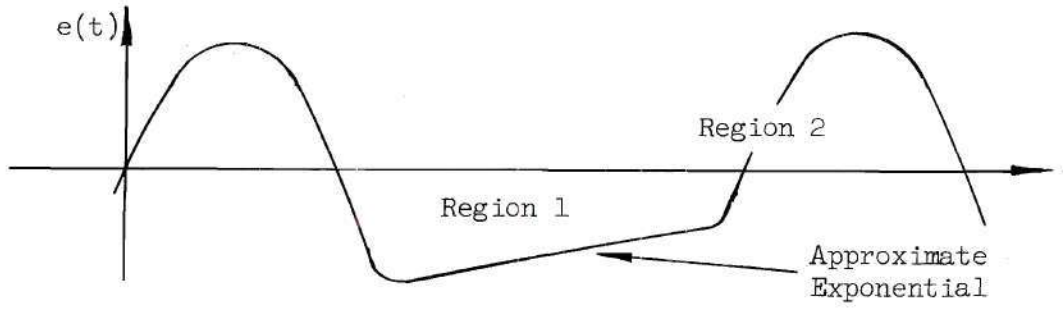

Figure 51. Relaxation Oscillation.

phenomenon which could possibly find some practical application.

CHAPTER V

SUMMARY AND CONCLUSIONS

It has been the purpose of this investigation to obtain the solution to a nonlinear differential equation describing a tunnel diode negative resistance oscillator. The characteristic of the solution upon which greatest attention has been focused is the waveshape of the steady-state output of the oscillator.

Some background material was given in Chapter II describing the actual test circuit which was used. Following this there were three forms of linear and quasi-linear analysis given in order to explain the fundamental mechanism of a negative resistance oscillator. The discussion then considered the nonlinear character of the tunnel diode and the nonlinear differential equation describing the oscillator was derived. A graphical approach for obtaining the solution to the equation was then discussed with phase-plane analysis chosen as the technique to be used.

Since numerical phase-plane analysis is laborious and time-consuming, it was decided to program the nonlinear equation on an analog computer. This resulted in a solution consisting of the trajectory in the phase-plane and the instantaneous waveform being presented simultaneously in graphical form by the computer output.

Chapter III discussed the procedure and instrumentation involved in programming the equation on the computer in terms of phase-plane variables and the design of a function generator which incorporates the tunnel diode itself to simulate the nonlinear function which is contained

in the equation. Also presented in Chapter III was a definition of the circuit parameters whose influences on the waveshape were to be studied. These parameters were:

(a) Impedance Level, $Z \triangleq K_z^2 Z_b$ with the constant K_z to be varied.

(b) The circuit $Q \triangleq K_z/K_r \, Q_b$ with the constant K_r used to vary Q while holding the impedance level of the circuit (or K_z) constant.

(c) The point at which the diode was biased which controlled the magnitude of the negative incremental conductance offered by the tunnel diode.

Chapter IV presents the experimental results obtained from a large number of solutions to the oscillator equation for many different combinations of the circuit parameters. The role of each parameter in the overall circuit behavior and its influence on the output waveshape was discussed with the aid of several quasi-linear techniques, and an attempt was made to explain the influence of each circuit parameter by more than one technique. The conclusions reached were that the waveshape is improved by:

(a) Lowering the impedance level (decreasing K_z) when the circuit Q (K_z/K_r ratio) and bias point (magnitude of G_d) are fixed.

(b) Lowering the circuit Q (by increasing K_r) when the impedance level and bias are fixed.

(c) Varying the bias so as to decrease the magnitude of G_d when the impedance level and circuit Q are fixed.

During the course of this work there were simplifying assumptions made to facilitate forming a model for the oscillator from which the non-linear equation was derived. In particular, it was assumed that the series resistance and inductance of the diode were negligible. A more detailed analysis would have to refrain from this assumption since in some cases the series resistance of the diode might be as large or larger than that of the coil in the tank circuit. Also, as the frequency at which the tunnel diode might find application is raised, the assumption of negligible series inductance would be unwarranted.

Some interesting phenomena which came to light during the experimental work are:

(a) The circuit parameters have an effect on the transient build up of oscillation. In some cases, the steady-state amplitude was reached almost immediately while in others the build up was very slow with an almost linear envelope.

(b) The oscillator is self-starting in some cases only if the initial conditions in the circuit are above some critical value.

(c) The oscillator displayed amplitude hysteresis for some combinations of the circuit parameters.

(d) The waveshape in the relaxation mode can be made to exhibit an almost linear ramp during a portion of the cycle with the remainder of the cycle being almost sinusoidal.

Each of the characteristics mentioned above could potentially be used in practical applications, and an investigation of any one of these could prove both interesting and useful.

A P P E N D I C E S

APPENDIX A

TYPICAL DIODE PARAMETERS
(GE Type 1N2940)

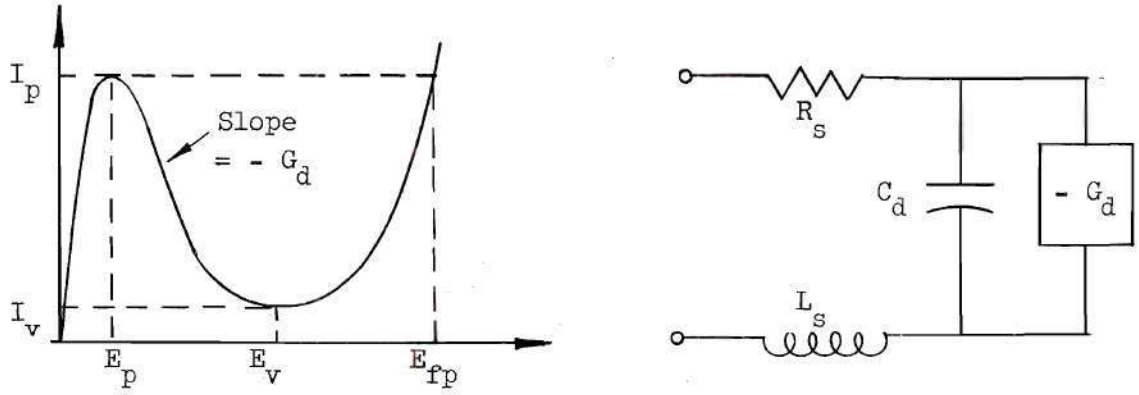

Figure A1. Typical Static Characteristic Curve and Equivalent Circuit.

Table A1. Typical Tunnel Diode Parameter Values.

Parameter	Symbol	Typical Value	Units
Peak Point Current	I_p	1.0	ma
Valley Point Current	I_v	0.1	ma
Peak Point Voltage	E_p	70	mv
Valley Point Voltage	E_v	350	mv
Forward Peak Point Current Voltage	E_{fp}	500	mv
Negative Conductance	$-G_d$	-6.6×10^{-3}	mhos
Diode Capacitance	C_d	5.0	μμf
Series Inductance	L_s	6×10^{-9}	hy
Series Resistance	R_s	1.5	ohm

APPENDIX B

SCALING PROCEDURE FOR EQUATION (73)

Choice of Base Parameter Values

The base values chosen for the circuit parameters were those shown in Figure 5 of Chapter II. Taking into account the fact that the total capacity is the sum of the diode capacitance and the external tank capacitance, the base values are

$$C_b = 1755 \ \mu\mu f \ , \tag{B1}$$

$$L_b = 15 \ \mu hy \ , \tag{B2}$$

and

$$R_b = 1 \ ohm \ . \tag{B3}$$

Rewriting equation (73) in terms of the base values yields

$$\frac{de}{dt} + \left(\frac{K_r}{K_z} \right) 6.66 \times 10^4 \, e + 38 \times 10^{12} \int e \, dt \tag{B4}$$

$$+ (K_z) 5.7 \times 10^8 \, f(e) + (K_r) 38 \times 10^{12} \int f(e) dt = 0.$$

Time Scaling

Time scaling of equation (B4) must take into account the characteristics of the equipment used to record the solution. In particular, the maximum plotting speeds of the X-Y recorder and Sanborn recorder must

be considered if the solution is to be plotted accurately.

The frequency response of the Sanborn recorder is much higher than that of the Moseley Autograph X-Y recorder; therefore, if the problem is scaled within the capabilities of the X-Y recorder, an accurate plot of the solution can be expected with both instruments.

In recording the data for this thesis, it was desirable to obtain phase-plane plots which, if perfect circles, would be on the order of 6 inches in maximum diameter. The limit-cycle is then approximately 19 inches in circumference at the maximum. Since the limit-cycle is traversed with each cycle of the oscillation, this must be used as the basis for the choice of time scale. The period of oscillation is approximately 1 micro-second. The maximum tracking speed of the X-Y recorder is on the order of 11 inches per second. The change in time scale was therefore chosen as

$$T = 5 \times 10^{6} t \ , \qquad (B5)$$

where T indicates computer or machine-time, and t indicates actual oscillator time. The choice of time-scaling indicated in equation (B5) makes 5 seconds of machine-time correspond to 1 microsecond in the oscillator. The limit-cycle would then be traced out every 5 seconds, corresponding to a tracking speed of less than 4 inches per second which is well within the limits of the X-Y recorder.

Upon making the substitution of equation (B5) in the differential equation (B4), the derivatives and differentials become

$$\frac{d}{dt} = \frac{d}{dT/5 \times 10^{6}} = 5 \times 10^{6} \frac{d}{dT} \ , \qquad (B6)$$

and

$$dt = \frac{dT}{5 \times 10^6} . \tag{B7}$$

The time-scaled equation is then

$$\frac{de}{dT} + \left(\frac{K_r}{K_z} \right) 0.01332\, e + 1.52 \int e\, dT \tag{B8}$$

$$+ (K_z)114\, f(e) + (K_r)1.52 \int f(e)dT = 0 .$$

The natural frequency, after time-scaling, is now

$$\omega_T = \frac{1}{5 \times 10^6} \frac{1}{\sqrt{L_b C_b}} = 1.232 \frac{\text{radians}}{\text{machine-sec}} . \tag{B9}$$

Amplitude Scaling

Proper amplitude scaling requires a knowledge of the maximum values assumed by the problem variable and its derivatives. Since the solution in this case was unknown, these quantities were estimated from a knowledge of the physical system under investigation and by trial and error.

A preliminary check of the oscillator output revealed that amplitudes of at least 220 mv could be expected. A useful assumption in estimating the maximum value of the derivatives is that the output is sinusoidal. Since there is no way of ruling out, in advance, output amplitudes greater than 220 mv, a conservative approximation for the output is

$$e(t) = 300 \sin \left(\frac{t}{\sqrt{L_b C_b}} \right) \text{ mv} . \qquad \text{(B10)}$$

The maximum of the derivative is then

$$\left(\frac{de}{dt} \right)_{max} = \frac{300}{\sqrt{L_b C_b}} = 1850 \times 10^6 \text{ mv/sec} , \qquad \text{(B11)}$$

and the maximum of the time-scaled derivative is

$$\left(\frac{de}{dT} \right)_{max} = \frac{1850 \times 10^6}{5 \times 10^6} = 370 \frac{\text{mv}}{\text{machine-sec}} . \qquad \text{(B12)}$$

Considering the diode characteristic, a conservative estimate of the maximum value assumed by f(e) might be 0.5 ma. The estimated maxima of the variables in equation (B8) are then

$$\left.\begin{aligned} \left(\frac{de}{dT}\right)_{max} &= 370 \frac{\text{mv}}{\text{machine-sec}} , \\ (e)_{max} &= 300 \text{ mv} , \\ \text{and} \qquad f(e)_{max} &= 0.5 \text{ ma} . \end{aligned}\right\} \qquad \text{(B13)}$$

Following the procedure of Johnson (11), it is convenient at this point to define a machine unit as 1 volt and to define for each variable a scale factor of the form

$$a \triangleq \frac{1 \text{ machine unit}}{1 \text{ physical unit}} = \frac{1 \text{ volt}}{1 \text{ physical unit}} . \qquad \text{(B14)}$$

Multiplying each problem variable by its appropriate scale factor then changes the problem units to the units of volts. This method of scaling

is advantageous since all the scale factors are numerically unity, and the machine equation remains exactly equivalent in form to that of the physical equation.

Under this scheme, the following correspondence between the problem variables and the machine variable (volts) is obtained:

$$\left.\begin{aligned} 1\ \frac{\text{millivolt}}{\text{machine-sec}} &= 1\ \text{volt} \\ 1\ \text{millivolt} &= 1\ \text{volt} \\ 1\ \text{milliamp} &= 1\ \text{volt}\ . \end{aligned}\right\} \qquad \text{(B15)}$$

This means that if the quantity ($\frac{de}{dT}$) in equation (B8) ranges between ± 370 mv machine-sec as assumed, then the voltage on the computer which represents this quantity will vary between ± 370 volts. If the variable e varies between ± 300 mv as assumed, the voltage on the computer which represents this variable will range between ± 300 volts. Likewise, the voltage on the computer which corresponds to the function f(e) will vary between ± 0.5 volts.

The Berkley EASE Analogue Computer, which was used, utilizes amplifiers with a dynamic range of ± 100 volts. To place the range of the variables within the range of the amplifier outputs, equation (B8) must be multiplied through by an appropriate constant or scale factor. Before making this step, however, it is appropriate to discuss some of the characteristics of the problem at hand which influence the choice of scale factor.

For high accuracy, a problem should be amplitude-scaled so that the amplifier outputs vary over as wide a portion of their dynamic range

as possible, and low output ranges are usually avoided. In a nonlinear problem, as is the case here, this is usually very difficult to achieve when solutions are to be obtained with many different values assigned to the equation coefficients. In this case, it is very difficult to predict (short of a graphical solution) what effect the equation coefficients have on the range of the problem variables.

Another problem which must be dealt with in the amplitude-scaling of equation (B8) is the relative inconsistency in the magnitudes of the coefficients. Relatively speaking, some are very large while others are very small. Coupled with the fact that the range of the voltage representing f(e) is very small compared with that of the other machine variables, it is inevitable that the problem be run with some parts of the computer operating at very low voltage levels.

This situation is a consequence of the fact that the tunnel diode, which is a low impedance device, must operate into a parallel resonant circuit of relatively high impedance. This mismatch in impedance levels is a unique characteristic of the problem at hand and must be accepted even though it dictates a situation which is deemed incompatible with high accuracy in a computer solution.

For each value of K_r and K_z to be considered in taking data, the program of equation (B8) could be modified on a trial basis so as to make the most efficient use of the amplifier ranges, but this makes each data point effectively a problem in itself, and the time required to run sufficient data would be prohibitive. With this in mind, it was decided to program equation (B8) for relatively low voltage ranges, in particular limiting the amplifiers to a range of ± 20 volts. With this low range,

the problem variables can go far beyond the original estimates before the amplifiers reach the absolute maximum of ± 100 volts and necessitate a major change in the program.

Transposing and using the dot notation for the time derivative, equation (B8) may be rewritten as

$$(\dot{e}) = -\left(\frac{K_r}{K_z}\right) 0.01332(e) - 1.52 \int e \, dT \qquad \text{(B16)}$$

$$- (K_z)\, 114\, f(e) - (K_r)\, 1.52 \int f(e)\, dT \, .$$

To limit the amplifiers to ± 20 volts, appropriate outputs would be $(\frac{\dot{e}}{20})$ and $(\frac{e}{20})$. Multiplying equation (B16) by (1/20) yields

$$(\tfrac{\dot{e}}{20}) = -\left(\frac{K_r}{K_z}\right) 0.01332\, (\tfrac{e}{20}) - 1.52 \int (\tfrac{e}{20})\, dT \qquad \text{(B17)}$$

$$- (K_z)\, \tfrac{114}{20}\, f(e) - (K_r)\, \tfrac{1.52}{20} \int f(e)\, dT \, .$$

Under the scheme of assigning the machine variables, as denoted by equation (B15) a 1 ma change in diode current corresponds to a change of 1 volt in the computer voltage representing f(e). The function generator, however, has a built-in gain factor so that a 1 ma change in diode current actually produces a change of 5 volts at the output. To conform to the assignment of the computer variables in equation (B15), the output of the function generator is now labeled (5f), indicating that a 1 ma change in diode current produces a 5 volt change in the corresponding computer variable. Making the appropriate change in equation (B17) yields as the final form of the computer equation,

$$\left(\frac{\dot{e}}{20}\right) = -\left(\frac{K_r}{K_z}\right) 0.01332 \left(\frac{e}{20}\right) - 1.52 \int \left(\frac{e}{20}\right) dT \qquad \text{(B18)}$$

$$- (K_z)\, 1.14\, (5f) - (K_r)\, 0.0152 \int (5f)\, dT.$$

The detailed computer program for equation (B18) with $K_r = K_z = 1$ is shown in Figure B1.

A word of explanation about the settings of potentiometers 2 and 6 is appropriate at this point. As pointed out in the discussion of the function generator, the voltage fed to its input must be reduced to a millivolt level at the tunnel diode. For instance, if the computer variable e assumes the value 300 volts, the corresponding voltage applied to the tunnel diode must be 300 millivolts. If the computer variable takes on a value of 300 volts, then the output of amplifier 4 is 15 volts. The gain factor through amplifier 16 is 1/10; therefore, potentiometer 2 must be set at 0.2 to produce a voltage of 300 mv at the tunnel diode. That is,

$$\left(\frac{e}{20}\right) \times (\text{Pot. No. 2}) \times \left(\frac{1}{10}\right) = \qquad \text{(B19)}$$

$$15 \times \frac{2}{10} \times \frac{1}{10} = 300 \times 10^{-3} = 300 \text{ mv} .$$

The output of amplifier 11 is $\left(\frac{\dot{e}}{20}\right)$, but to plot the solution in the normalized phase-plane an input $(\nu/20)$ is required for the Y-axis of the X-Y recorder. From the definition,

$$\left(\frac{\nu}{20}\right) = \frac{1}{\omega_T} \left(\frac{\dot{e}}{20}\right) = 0.812 \left(\frac{\dot{e}}{20}\right) . \qquad \text{(B20)}$$

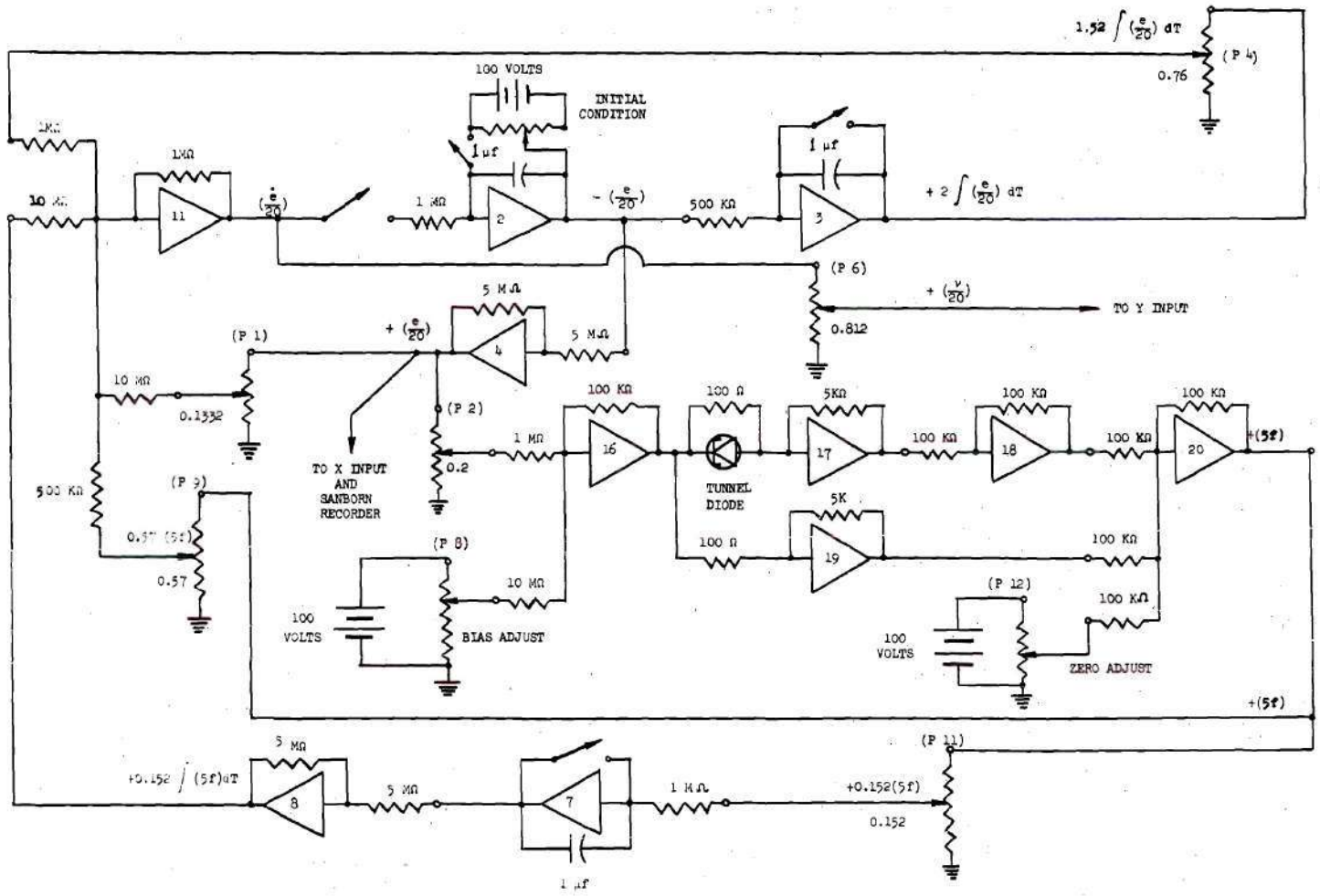

Figure B1. Scaled Computer Program for Equation (B18) for $K_z = 1$, $K_r = 1$.

Therefore, to plot solutions in the normalized phase-plane, the output of amplifier 11 must be fed to a potentiometer set at 0.812 before being fed to the recorder input.

With this scaling arrangement, a value of 15 volts for the computer output labeled $(v/20)$ corresponds to a value of 300 volts for the computer variable v and, hence, a value of 300 mv for the actual v of the oscillator. Likewise, a value of 15 volts for the computer output labeled $(e/20)$ corresponds to a value of 300 volts for the computer variable e and, hence, a value of 300 mv for the actual oscillator output voltage.

Changing the Problem Variables

To study the effects of changing the bias, Q, or impedance level, the corresponding changes must be made in the computer program of Figure B1.

Changing the point at which the diode is biased (and hence the origin for the function f(e)) is very simple. Since the outputs of the amplifiers are metered, all that is required is that potentiometer 8 be adjusted until the output of amplifier 16 reaches the desired bias voltage. The output of amplifier 20 is then brought to zero by adjusting potentiometer 12. Following this procedure, the origin of the function f(e) may be fixed at any point on the diode characteristic.

Changing the Q and impedance level will change the values of K_r and K_z and hence change the overall coefficients of the terms involving these factors. Note, however, that the coefficient values involving (K_r/K_z), (K_z), and (K_r) are fixed by adjusting potentiometers 1, 9, and 11 respectively along with their respective input resistances to amplifier 11. For example, suppose the Q and impedance level are picked in

such a manner that $K_r = 25$ and $K_z = 2$. Then

$$\left(\frac{K_r}{K_z} \right) 0.01332 = 0.1665 , \qquad (B21)$$

and potentiometer 1 is changed from 0.1332 to 0.1665 and the input resistance to amplifier 11 changed from 10 M to 1 M. Likewise

$$(K_z)\ 1.14 = 2.28 , \qquad (B22)$$

and potentiometer 9 is changed from 0.57 to 0.228 and the input resistance to amplifier 11 changed from 500 KΩ to 100 KΩ. Finally

$$(K_r)\ 0.0152 = 0.38 , \qquad (B23)$$

and potentiometer 11 is changed from 0.152 to 0.38 and the input resistance to amplifier 11 changed from 10 MΩ to 1 MΩ. In this manner, the solution to the oscillator equation may be found for many combinations of bias, Q, and impedance level.

BIBLIOGRAPHY

1. Van der Pol, B., "The Nonlinear Theory of Electric Oscillations," Proceedings of the Institute of Radio Engineers, Volume 22, No. 9, 1934, pp. 1051 - 1086.

2. Docherty, I. S., and R. E. Aitchison, "Waveforms in Tunnel Diode Oscillators," Proceedings of the Institute of Radio Engineers, (Australia) May 1962, pp. 304-310.

3. Lowry, H. R., Giorgis, J., and E. Gottlieb, Tunnel Diode Manual, Semiconductor Products Department, General Electric Company, 1st Ed., Liverpool, New York, 1961, p. 33.

4. Ibid., p. 34.

5. Reich, H. J., Functional Circuits and Oscillators, Princeton, New Jersey: D. Van Nostrand Company, Inc., 1961, pp. 100 - 103.

6. Edson, W. A., Vacuum-Tube Oscillators, New York: John Wiley and Sons, Inc., 1953, pp. 18 - 20.

7. Strauss, Leonard, Wave Generation and Shaping, New York: McGraw-Hill Book Company, Inc., 1960, pp. 492-499.

8. Truxal, John G., Control System Synthesis, New York: McGraw-Hill Book Company, Inc., 1955, Chapter 11, pp. 613-645.

9. Cunningham, W. J., Introduction to Nonlinear Analysis, New York: McGraw-Hill Book Company, Inc., 1958, Chapter 3, pp. 28-39.

10. Ibid., p. 35.

11. Johnson, Clarence L., Analog Computer Techniques, New York: McGraw-Hill Book Company, Inc., 1956, Chapter 3, pp. 20-42.